Bioorganic Chemistry 92 (2019) 103202

Contents lists available at ScienceDirect

Bioorganic Chemistry

journal homepage: www.elsevier.com/locate/bioorg

Novel 3,4-dihydro-4-oxoquinazoline-based acetohydrazides: Design, synthesis and evaluation of antitumor cytotoxicity and caspase activation activity

Le Cong Huan[a,e], Phuong-Thao Tran[a], Cao Viet Phuong[a], Phan Huy Duc[a], Duong Tien Anh[a], Pham The Hai[a], Le Thi Thu Huong[b], Nguyen Thi Thuan[a], Hye Jin Lee[c], Eun Jae Park[c], Jong Soon Kang[d], Nguyen Phuong Linh[f], Tran Trung Hieu[f], Dao Thi Kim Oanh[a,*], Sang-Bae Han[c,*], Nguyen-Hai Nam[a,*]

[a] Hanoi University of Pharmacy, 13-15 Le Thanh Tong, Hanoi, Viet Nam
[b] School of Medicine and Pharmacy, Hanoi National University, 144 Xuan Thuy, Hanoi, Viet Nam
[c] College of Pharmacy, Chungbuk National University, 194-31, Osongsaengmyung-1, Heungdeok, Cheongju, Chungbuk 28160, Republic of Korea
[d] Bio-Evaluation Center, Korea Research Institute of Bioscience and Biotechnology, Cheongju, Chungbuk 28116, Republic of Korea
[e] Thai Binh University of Medicine and Pharmacy, Thai Binh City, Viet Nam
[f] Hanoi Amsterdam High School, Hanoi, Viet Nam

ARTICLE INFO

Keywords:
Acetohydrazides
Quinazolin-4(3*H*)-one
Cytotoxicity
Caspase activation
Apoptotic inducers

ABSTRACT

In search for novel small molecules with antitumor cytotoxicity via activating procaspase-3, we have designed and synthesized three series of novel (E)-*N'*-benzylidene-4-oxoquinazolin-3(4*H*)-yl)acetohydrazides (**5a-j, 6a-h,** and **7a-h**). On the phenyl ring ò the benzylidene part, three different substituents, including 2-OH-4-OCH_3, 4-OCH_3, and 4-$N(CH_3)_2$, were introduced, respectively. Biological evaluation showed that the acetohydrazides in series **5a-j**, in which the phenyl ring of the benzylidene part was substituted by 2-OH-4-OCH_3 substituent, exhibited potent cytotoxicity against three human cancer cell lines (SW620, colon; PC-3, prostate; NCI-H23, lung). Most of the compounds, in this series, especially compounds **5c, 5b** and **5h,** also significantly activated caspase-3 activity. Among these, compound **5c** displayed 1.61-fold more potent than PAC-1 as caspase-3 activator. Cell cycle analysis showed that compounds **5b**, **5c**, and **5h** significantly arrested the cell cycle in G1 phase. Further apoptotic studies also demonstrated compounds **5b**, **5c**, and **5h** as strong apoptotic cell death inducers. The docking simulation studies showed that these compounds could activate procaspase *via* chelating Zn^{2+} ion bound to the allosteric site of the zymogen.

1. Introduction

Cancer is characterized by uncontrol growth and rapid proliferation of abnormal cells, which are able to surpass apoptotic response by different mechanisms [1,2]. Targeting apoptosis, has therefore, become one of the attractive approaches nowadays for the design and development of new anticancer agents [3]. With the advances in cancer molecular biology, various proteins involving cellular apoptotic pawthway, such as p53, XIAP, Bcl-2, BAX, BIM, to name a few, have been identified [2,3]. A number of small molecules targeting these proteins (e.g. tenovin-1, a p53 disruptor; GDC-0152, an inhibitor of XIAP; or ABT-199, a Bcl-2′s inhibitor) have been shown to effectively induce apoptosis, thus leading to the death of cancer cells [4–6].

In addition, different enzymes are also involved in regulation of cellular apoptosis. Among these, caspases with at least fourteen members (caspases 1–14), constitute a large family of cysteine proteases enzymes with important role in the initiation and execution of apoptosis [7]. Among these, caspase-3, which exists as a low activity zymogen in cells, known as procaspase-3, is one of the key enzymes involved in the apoptotic process [7]. Procaspase-3 is found overexpressed in various human cancers (e.g. colon cancer, lung cancer, melanoma, hepatoma, breast cancer, lymphoma, and neuroblastoma) [7–12]. It has been demonstrated that activation of procaspase-3 by appropriate small molecules effectively restores apoptosis in cancer cells [13–16]. Since procaspase-3 is overexpressed in various cancer cells, it is expected that targeting procaspase-3 would be more

* Corresponding authors.
E-mail addresses: shan@cbnu.ac.kr (S.-B. Han), namnh@hup.edu.vn (N.-H. Nam).

https://doi.org/10.1016/j.bioorg.2019.103202
Received 23 April 2019; Received in revised form 11 August 2019; Accepted 13 August 2019
Available online 14 August 2019

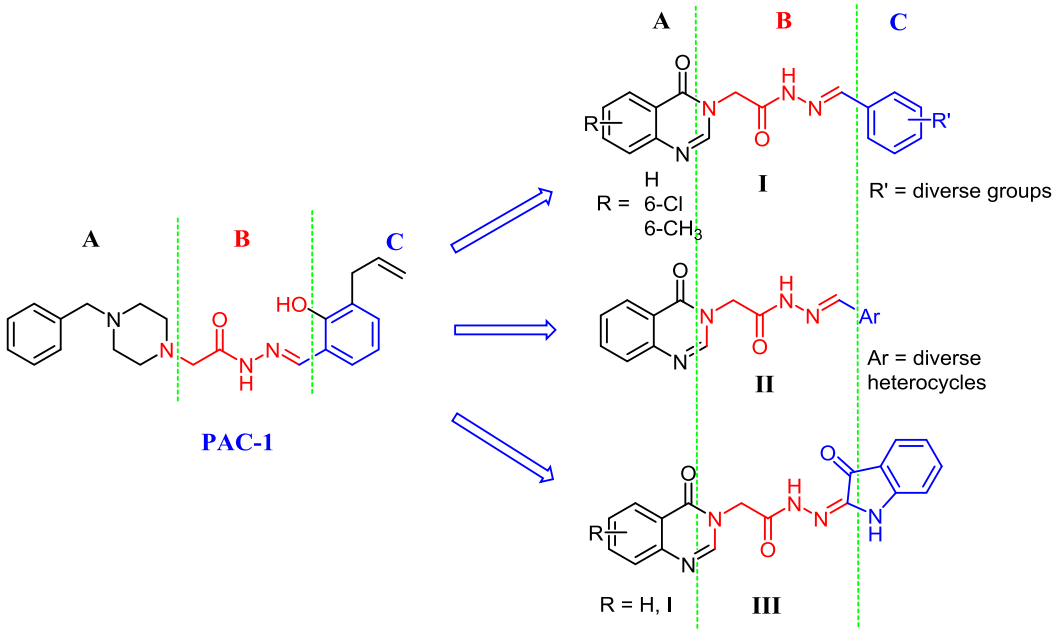

Fig. 1. Structures of PAC-1 and some previously designed 4-oxoquinazoline-based acetohydrazides.

advantageous in comparison to targeting direct apoptotic proteins.

PAC-1, the first procaspase activating compound (Fig. 1) reported recently, has been shown to have very promising *in vivo* antitumor activity profile in several xenografted models [7,14]. Studies on the structure-activity relationships of PAC-1 indicated that the ortho-hydroxy-*N*-acylhydrazone functionality (B-region, Fig. 1) formed a strong complex with zinc ion and played vital role for its procaspase activating and anticancer activity [15,16]. In our previous research to develop novel small molecules activating caspases we have designed, synthesized and evaluated a series of quinazoline-4(3*H*)-one-based acetohydrazides (Fig. 1) [17,18]. Structure-activity relationships regarding the substituents on the phenyl part of the structure has been investigated and three substituents, including 2-OH-4-OCH_3, 4-OCH_3, and 4-N$(CH_3)_2$ (Fig. 2), were found to be the most favorable for bioactivity. In this study we decided to further optimize the substituents on the quinazoline-4(3*H*)-one moiety (Fig. 2) in an attempt to obtain more potent candidates for further development.

2. Materials and methods

2.1. Chemistry

Thin layer chromatography which was performed using Whatman® 250 µm Silica Gel GF Uniplates and visualized under UV light at 254 nm, was used to check the progress of reactions and preliminary evaluation of compounds' homogeneity. Melting points were measured using a Gallenkamp Melting Point Apparatus (LabMerchant, London, United Kingdom) and are uncorrected. Purification of compounds was carried out using crystallization methods and/or open silica gel column flash chromatography employing Merck silica gel 60 (240 to 400 mesh) as stationary phase. Nuclear magnetic resonance spectra (^{1}H NMR) were recorded on a Bruker 500 MHz spectrometer with DMSO-d_6 as solvent unless otherwise indicated. Tetramethylsilane was used as an internal standard. Chemical shifts are reported in parts per million (ppm), downfield from tetramethylsilane. Mass spectra with different ionization modes including electron ionization (EI), Electrospray ionization (ESI), were recorded using PE Biosystems API2000 (Perkin Elmer, Palo Alto, CA, USA) and Mariner® (Azco Biotech, Inc. Oceanside, CA, USA) mass spectrometers, respectively. The elemental (C, H, N) analyses were performed on a Perkin Elmer model 2400 elemental

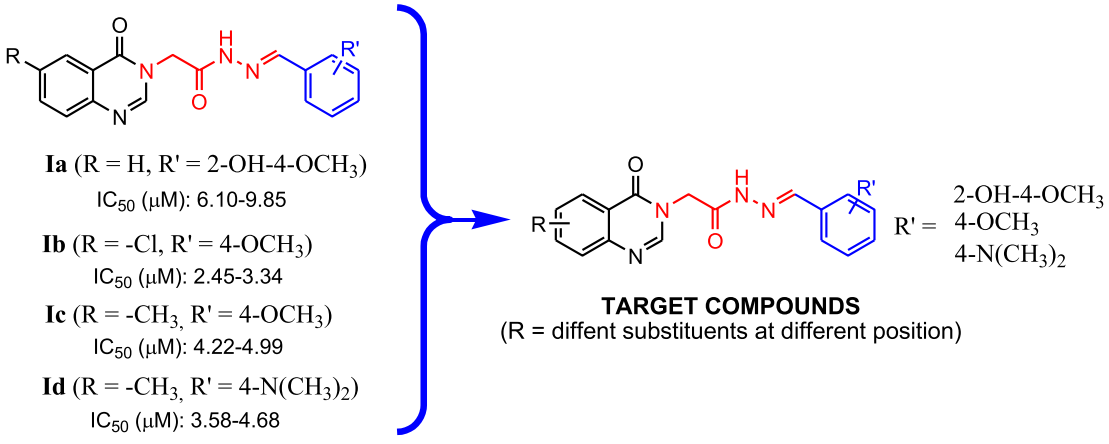

Fig. 2. Cytotoxicity of some previously designed 4-oxoquinazoline-based acetohydrazides and further design of 4-oxoquinazoline-based acetohydrazides.

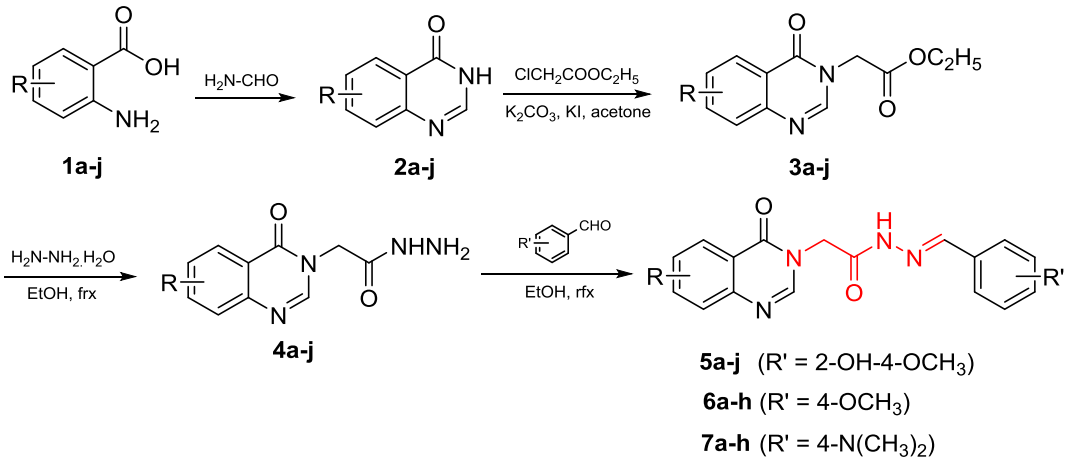

Scheme 1. Synthesis of acetohydrazides incorporating quinazolin-4(3*H*)-one (**5a-j, 6a-h, 7a-h**). *Reagents and conditions:* (a) H_2N-CHO, 120 °C, 3 h; (b) ethyl chloroacetate, KI, K_2CO_3, acetone, 60 °C, 3.5 h; (c) $N_2H_4{\cdot}H_2O$, EtOH, reflux; (d) Ar-CHO or isatin der., AcOH conc., EtOH, reflux.

analyzer. All reagents and solvents were purchased from Aldrich or Fluka Chemical Corp. (Milwaukee, WI, USA) or Merck unless noted otherwise. Solvents were used directly as purchased unless otherwise indicated.

The synthesis of acetohydrazides incorporating quinazolin-4(3*H*)-one (**5–7**) was carried out as illustrated in Scheme 1. Details are described below.

The mixtures of anthranilic acid or respective 5-substituted-2-aminobenzoic acid (**1**) (1 mmol) and an excess of formamide (10 mmol) in a round-bottom flask were heated at 120 °C with stirring for 3–5 h. The reaction was checked by TLC. After the starting materials completely disappeared, the resulting mixtures were cooled to room temperature and then poured into ice-cold water. The light or dark brown precipitates were formed. The precipitates were filtered and washed three times with water (20 mL each) and dried to give quinazoline-4(3*H*)-one derivatives (**2**). These intermediates were used for the next step without further purification.

To a solution of each respective quinazoline-4(3*H*)-one intermediate (**2**) (1 mmol) in acetone (10 mL) were added K_2CO_3 (207 mg, 1.5 mmol). The resulting mixture was heated at 80 °C with stirring for 30 min. KI (16.6 mg, 0.1 mmol) was added and after stirring for further 15 min, ethyl chloroacetate (0.13 mL, 1.2 mmol) diluted with acetone (1 mL) was dropwise added into the mixture. The reaction mixture was further stirred at 60 °C for 3 h. After the reaction completed, the resulting mixture was cooled, poured into ice-cold water. The brown solids were formed, filtered and dried to give the corresponding ethyl 2-(4-oxoquinazolin-3-(4*H*)-yl)acetate derivatives **3**.

To a respective solution of the ester **3** (0.5 mmol) in ethanol (10 mL) was added slowly 0.12 mL of hydrazine monohydrate (2.5 mmol). The mixture was stirred at room until the starting material was completely consumed. The white precipitates were formed, filtered, and washed with cold-ethanol (3 times). The white solids (the hydrazides **4**) were collected, dried under vacuum and used for the next step without further purification.

Each of the hydrazides **4** (0.5 mmol) was dissolved in ethanol (20 mL), then 2 drops of concentrated acetic acid, followed by benzaldehyde or isatine derivatives (1.0 mmol) were added. The mixture was refluxed until the reaction completed. The precipitates were formed, filtered, and washed with ethanol (3 times). The white solids were collected, dried under vacuum and re-crystalised in ethanol or column chromatography (DCM/MeOH) to obtain the desired products (**5–7**). The physicochemical and spectral data for compounds **5a**, **6a**, **6c**, **6h**, and **7c** had been reported previously [17].

*2.1.1. (E)-N′-(2-Hydroxy-4-methoxybenzylidene)-2-(7-methyl-4-oxoquinazolin-3(4H)-yl)acetohydrazide (**5b**)*

White solid; Yield: 65%. mp: 184–185 °C. R_f = 0.59 (DCM: MeOH = 14: 1). *IR (KBr, cm^{-1}):* 3271 (NH); 3181 (OH); 3066 (CH aren); 2968, 2897, 2839 (CH, CH_2); 1682 (C=O); 1663 (C=N); 1612 (C=C). *^{1}H NMR (500 MHz, DMSO-d_6, ppm)*: δ 11.99, 11.62 (2s, 0.5H, 0.5H, OH); 11.27, 10.21 (2s, 0.5H, 0.5H, CONH); 8.37–8.29 (m, 2H, N = C<u>H</u>, H_2); 8.05 (dd, *J* = 8.0 Hz, *J′* = 2.5 Hz, 1H, H_5); 7.67 (d, *J* = 8.5 Hz, 1H, H_6); 7.54 (d, *J* = 4.5 Hz, 1H, H_8); 7.40 (d, *J* = 8.0 Hz, 1H, $H_{6'}$); 6.54–6.50 (m, 2H, $H_{3'}$, $H_{5'}$); 5.17, 4.78 (2s, 1.0H, 1.0H, N-C<u>H</u>$_2$-CO); 3.77 (d, *J* = 3.0 Hz, 3H, OC<u>H</u>$_3$); 2.49 (s, 3H, C<u>H</u>$_3$). *^{13}C NMR (125 MHz, DMSO-d_6, ppm):* δ 168.1, 163.5, 162.7; 162.5; 160.6; 159.7; 158.5; 149.2, 149.0, 148.7, 148.7, 148.5, 145.6, 145.5, 142.5, 131.4, 128.2, 127.4, 127.3, 126.4, 126.3, 119.6, 119.5, 113.5, 112.1, 107.0, 101.6, 101.4, 55.9, 55.8, 55.7, 47.8, 47.2, 21.8. HR-MS (ESI) *m/z* 365.1232 $[M-H]^-$. Anal. Calcd. For $C_{19}H_{18}N_4O_4$ (366.1328): C, 62.29; H, 4.95; N, 15.29. Found: C, 62.38; H, 5.11; N, 15.18.

*2.1.2. (E)-N′-(2-Hydroxy-4-methoxybenzylidene)-2-(6-methyl-4-oxoquinazolin-3(4H)-yl)acetohydrazide (**5c**)*

White solid; Yield: 60%. mp: 188–189 °C. R_f = 0.57 (DCM: MeOH = 14: 1). *IR (KBr, cm^{-1}):* 3181 (OH); 3069 (CH aren); 2986, 2918, 2851 (CH, CH_2); 1663 (C=N); 1624, 1605, 1566 (C=C). *^{1}H NMR (500 MHz, DMSO-d_6, ppm)*: δ 11.97, 11.60 (2s, 0.5H, 0.5H, OH); 11.26, 10.19 (2s, 0.5H, 0.5H, CONH); 8.37, 8.31 (2s, 0.5H, 0.5H, N = CH); 8.29 (d, *J* = 8.0 Hz, 1H, H_2); 7.96 (s, 1H, H_5); 7.70 (dd, *J* = 5.5 Hz, *J′* = 3.0 Hz, 1H, H_7); 7.68 (d, *J* = 2.5 Hz, 1H, H_8); 7.63 (dd, *J* = 8.5 Hz, *J′* = 5.5 Hz, 1H, $H_{6'}$); 6.54–6.48 (m, 2H, $H_{3'}$, $H_{5'}$); 5.17, 4.78 (2s, 1.0H, 1.0H, CH_2); 3.76 (s, 3H, OC<u>H</u>$_3$); 2.47 (s, 3H, C<u>H</u>$_3$). *^{13}C NMR (125 MHz, DMSO-d_6, ppm):* δ 168.1, 163.5, 162.7, 162.5, 160.7, 159.7, 158.5, 148.5, 148.3, 148.1, 146.6, 142.5, 138.4, 137.3, 136.3, 136.2, 131.4, 128.2, 127.6, 125.8, 125.7, 113.5, 112.1, 107.0, 101.6, 101.4, 55.8, 55.7, 47.9, 47.3, 21.3. HR-MS (ESI) *m/z* 365.1255 $[M-H]^-$. Anal. Calcd. For $C_{19}H_{18}N_4O_4$ (366.1328): C, 62.29; H, 4.95; N, 15.29. Found: C, 62.18; H, 4.83; N, 15.37.

*2.1.3. (E)-2-(6,7-Dimethoxy-4-oxoquinazolin-3(4H)-yl)-N′-(2-hydroxy-4-methoxybenzylidene)acetohydrazide (**5d**)*

White solid; Yield: 58%. mp: 197–198 °C. R_f = 0.59 (DCM: MeOH = 14: 1). *IR (KBr, cm^{-1}):* 3161 (OH); 3084 (CH aren); 2963, 2901, 2841 (CH, CH_2); 1692 (C=O); 1645 (C=N); 1603, 1501 (C=C). *^{1}H NMR (500 MHz, DMSO-d_6, ppm)*: δ 11.97, 11.60 (2s, 0.5H, 0.5H, OH); 11.28, 10.19 (2s, 0.5H, 0.5H, CON<u>H</u>); 8.37–8.25 (m, 2H, N = C<u>H</u>, H_2); 7.67, 7.47 (2d, *J* = 8.5 Hz, 0.5H, 0.5H, $H_{6'}$); 7.47 (s, 1H, H_5); 7.20 (s, 1H, H_8); 6.52 (s, 1H, $H_{5'}$); 6.48 (s, 1H, $H_{3'}$); 5.16, 4.77 (2s, 0.5H, 0.5H, NC<u>H</u>$_2$CO); 3.94, 3.89, 3.77 (3 s, 9H, OC<u>H</u>$_3$). *^{13}C NMR (125 MHz,*

DMSO-d_6, ppm): δ 168.2, 163.6, 162.6, 162.5, 160.1, 159.7, 158.4, 155.1, 155.0, 149.3, 149.2, 148.5 ,146.5, 147.5, 144.7, 142.5, 131.4, 128.2, 115.1, 115.0, 113.5, 112.1, 108.5, 107.0, 105.6, 105.5, 101.6, 101.4, 56.5, 56.2, 55.8, 47.8, 47.2. HR-MS (ESI) *m/z* 454.1714 $[M + H + CH_3CN]^+$. Anal. Calcd. For $C_{20}H_{20}N_4O_6$ (412.1383): C, 58.25; H, 4.89; N, 13.59. Found: C, 58.37; H, 4.95; N, 13.48.

2.1.4. (E)-2-(7-Fluoro-4-oxoquinazolin-3(4H)-yl)-N′-(2-hydroxy-4-methoxybenzylidene)acetohydrazide (**5e**)

White solid; Yield: 64%. mp: 186–187 °C. R_f = 0.54 (DCM: MeOH = 14: 1). *IR (KBr, cm^{-1}):* 3176 (OH); 3076 (CH aren); 2976, 2905, 2839 (CH, CH_2); 1694 (C═O); 1667 (C═N); 1630, 1603, 1570 (C═C). *^{1}H NMR (500 MHz, DMSO-d_6, ppm)*: δ 11.97, 11.63 (2s, 0.4H, 0.6H, CONH); 11.24, 10.19 (2s, 0.4H, 0.6H, OH); 8.88 (s, 1H, H_2); 8.43, 8.42 (2s, 0.4H, 0.6H, N = CH); 8.23 (s, 1H, H_5); 7.67, 7.46 (2d, *J* = 8.5 Hz, 0.4H, 0.6H, $H_{6'}$); 7.55–7.53 (m, 2H, H_8, H_6); 6.53–6.48 (m, 2H, $H_{3'}$, $H_{5'}$); 5.18, 4.79 (2s, 1.2H, 0.8H, NCH_2CO); 3.77 (s, 3H, OCH_3). *^{13}C NMR (125 MHz, DMSO-d_6, ppm):* δ 162.7, 162.5, 161.1, 160.1, 159.7, 158.5, 150.8, 150.7, 150.5, 150.4, 148.6, 142.6, 133.2, 131.4, 129.8, 129.7, 128.1, 119.0, 116.4, 116.3, 116.2, 116.1, 113.5, 113.01, 113.0, 112.8, 112.1, 111.9, 107.6, 107.0, 101.6, 101.4, 56.0, 55.8, 55.7, 47.9, 47.4. HR-MS (ESI) *m/z* 369.0990 $[M-H]^-$. Anal. Calcd. For $C_{18}H_{15}FN_4O_4$ (370.1077): C, 59.38; H, 4.08; N, 15.13. Found: C, 59.47; H, 4.19; N, 15.09.

2.1.5. (E)-2-(6-Fluoro-4-oxoquinazolin-3(4H)-yl)-N′-(2-hydroxy-4-methoxybenzylidene)acetohydrazide (**5f**)

White solid; Yield: 62%. mp: 186–187 °C. R_f = 0.53 (DCM: MeOH = 14: 1). *IR (KBr, cm^{-1}):* 3198 (OH); 3063 (CH aren); 2899, 2839 (CH, CH_2); 1691 (C═O); 1663 (C═N); 1630, 1601, 1570 (C═C). *^{1}H NMR (500 MHz, DMSO-d_6, ppm)*: δ 11.96, 11.62 (2s, 0.4H, 0.6H, OH); 11.24, 10.18 (2s, 0.4H, 0.6H, CONH); 8.38, 8.29 (2s, 0.4H, 0.6H, N = CH); 8.37 (s, 1H, H_2); 7.85–7.76 (m, 3H, H_5, H_7, H_8); 7.67, 7.46 (2d, *J* = 9.0 Hz, 0.4H, 0.6H, $H_{6'}$); 6.54–6.47 (m, 2H, $H_{3'}$, $H_{5'}$); 5.19, 4.80 (2s, 1.2H, 0.8H, NCH_2CO); 3.77 (s, 3H, OCH_3).*^{13}C NMR (125 MHz, DMSO-d_6, ppm):* δ 167.9, 163.3, 162.7, 162.5, 160.1, 159.7, 158.5, 148.6, 148.4, 145.5, 142.6, 131.4, 130.7, 128.1, 123.5, 123.1, 113.5, 112.1, 111.3, 111.1, 107.0, 101.6, 101.4, 55.8, 55.7, 48.0, 47.5. HR-MS (ESI) *m/z* 369.0990 $[M-H]^-$. Anal. Calcd. For $C_{18}H_{15}FN_4O_4$ (370.1077): C, 59.38; H, 4.08; N, 15.13. Found: C, 59.27; H, 4.17; N, 15.21.

2.1.6. (E)-2-(7-Chloro-4-oxoquinazolin-3(4H)-yl)-N′-(2-hydroxy-4-methoxybenzylidene)acetohydrazide (**5g**)

White solid; Yield: 68%. mp: 189–190 °C. R_f = 0.57 (DCM: MeOH = 14: 1). *IR (KBr, cm^{-1}):* 3179 (OH); 3069 (CH aren); 2970, 2911, 2841 (CH, CH_2); 1697 (C═O); 1667 (C═N); 1632, 1603, 1570 (C═C). *^{1}H NMR (500 MHz, DMSO-d_6, ppm)*: δ 8.43, 8.27 (2s, 0.4H, 0.6H, CONH); 8.43, 8.37 (2s, 0.4H, 0.6H, N = CH); 8.41 (s, 1H, H_2); 8.29 (s, 1H, H_5); 7.93–7.90 (m, 1H, H_7); 7.79–7.76 (m, 1H, H_8); 7.67–7.46 (2d, *J* = 8.5 Hz, 0.6H, 0.4H, $H_{6'}$); 6.53–6.50 (m, 2H, $H_{3'}$, $H_{5'}$); 5.20, 4.81 (2s, 1.2H, 0.8H, NCH_2CO); 3.77 (s, 3H, OCH_3). *^{13}C NMR (125 MHz, DMSO-d_6, ppm):* δ 167.8, 163.3, 162.7, 162.5, 159.8, 158.6, 149.6, 149.4, 148.6, 147.3 , 142.6, 135.2, 135.1, 132.0, 131.9, 131.3, 130.1, 128.1, 125.5, 125.4, 123.1, 113.5, 112.1, 106.9, 101.6, 101.4 55.8, 55.7, 48.1, 47.5. MS (ESI) *m/z* 386.8 $[M + H]^+$. Anal. Calcd. For $C_{18}H_{15}ClN_4O_4$ (386.0782): C, 55.89; H, 3.91; N, 14.49. Found: C, 55.97; H, 3.46; N, 14.40.

2.1.7. (E)-2-(7-Bromo-4-oxoquinazolin-3(4H)-yl)-N′-(2-hydroxy-4-methoxybenzylidene)acetohydrazide (**5h**)

White solid; Yield: 67%. mp: 211–212 °C. R_f = 0.61 (DCM: MeOH = 14: 1). *IR (KBr, cm^{-1}):* 3190 (OH); 3065 (CH aren); 2984, 2911, 2837 (CH, CH_2); 1697 (C═O); 1670 (C═N); 1630, 1607, 1570 (C═C). *^{1}H NMR (500 MHz, DMSO-d_6, ppm)*: δ 11.98, 11.65 (2s, 0.4H, 0.6H, OH); 11.24, 10.20 (2s, 0.4H, 0.6H, CONH); 8.43, 8.42 (2s, 0.4H, 0.6H, H_2); 8.36, 8.28 (2s, 0.4H, 0.6H, N = CH); 8.25–8.24 (m, 1H, H_5); 8.03 (d, *J* = 8.5 Hz, 1H, H_7); 7.71–7.66 (m, 1H, H_8); 7.46 (d, *J* = 9.0 Hz, 1H, $H_{6'}$); 6.54–6.50 (m, 2H, $H_{3'}$, $H_{5'}$); 5.19, 4.80 (2s, 1.2H, 0.8H, NCH_2CO); 3.77 (s, 3H, OCH_3). *^{13}C NMR (125 MHz, DMSO-d_6, ppm):* δ 167.8, 163.2, 162.7, 162.5, 159.7, 158.5, 149.7, 149.6, 148.6, 147.6, 147.5, 142.5, 137.9, 131.3, 130.2, 128.6, 128.1, 123.5, 120.1, 113.5, 112.1, 107.0, 101.6, 101.4, 55.8, 55.7, 48.1, 47.6. MS (ESI) *m/z* 428.97 $[M-H]^-$. Anal. Calcd. For $C_{18}H_{15}BrN_4O_4$ (330.0277): C, 50.13; H, 3.51; N, 12.99. Found: C, 50.20; H, 3.59; N, 12.88.

2.1.8. (E)-N′-(2-Hydroxy-4-methoxybenzylidene)-2-(6-nitro-4-oxoquinazolin-3(4H)-yl)acetohydrazide (**5i**)

White solid; Yield: 55%. mp: 184–185 °C. R_f = 0.58 (DCM: MeOH = 14: 1). *IR (KBr, cm^{-1}):* 3179 (OH); 3069 (CH aren); 2982, 2903 (CH, CH_2); 1697 (C═O); 1668 (C═N); 1630, 1603, 1522 (C═C). *^{1}H NMR (500 MHz, DMSO-d_6, ppm)*: δ 11.98, 11.65 (2s, 0.4H, 0.6H, OH); 11.19, 10.18 (2s, 0.4H, 0.6H, CONH); 8.53 (d, *J* = 5.0 Hz, 1H, H_2); 8.44–8.43 (m, 1H, N = CH); 8.39–8.27 (m,3H, H_5, H_7, H_8); 7.65, 7.44 (2d, *J* = 8.5 Hz, 0.4H, 0.6H, $H_{6'}$); 6.51–6.45 (m, 2H, $H_{3'}$, $H_{5'}$); 5.21, 4.82 (2s, 1.2H, 0.8H, NCH_2CO); 3.74 (s, 3H, OCH_3). *^{13}C NMR (125 MHz, DMSO-d_6, ppm):* δ 163.0, 162.7, 162.5, 159.9, 159.7, 158.5, 151.7, 151.3, 151.1, 148.9, 148.6, 142.6, 131.3, 128.9, 128.1, 126.1, 122.9, 121.4, 121.3, 113.4, 112.1, 107.0, 101.6, 101.4, 55.8, 55.7, 48.2, 47.8. HR-MS (ESI) *m/z* 396.0969 $[M-H]^-$. Anal. Calcd. For $C_{18}H_{15}N_5O_6$ (397.1022): C, 54.41; H, 3.81; N, 17.63. Found: C, 54.53; H, 3.75; N, 17.74.

2.1.9. (E)-N′-(2-Hydroxy-4-methoxybenzylidene)-2-(7-nitro-4-oxoquinazolin-3(4H)-yl)acetohydrazide (**5j**)

White solid; Yield: 58%. mp: 185–186 °C. R_f = 0.57 (DCM: MeOH = 14: 1). *IR (KBr, cm^{-1}):* 3265 (NH); 3098 (CH aren); 3034, 2945, 2841 (CH, CH_2); 1722 (C═O); 1668 (C═N); 1629, 1609, 1570 (C═C). *^{1}H NMR (500 MHz, DMSO-d_6, ppm)*: δ 11.98, 11.60 (2s, 0.4H, 0.6H, OH); 11.12, 10.11 (2s, 0.4H, 0.6H, CONH); 8.78–8.76 (m, 1H, H_2); 8.53–8.50 (m, 2H, N = CH, H_5); 8.28, 8.20 (2s, 0.4H, 0.6H, H8); 7.86 (dd, *J* = 9.0 Hz, *J′* = 6.0 Hz, 1H, H6); 7.59, 7.37 (2d, *J* = 8.5 Hz, 0.4H, 0.6H, $H_{6'}$); 6.44–6.38 (m, 2H, $H_{3'}$, $H_{5'}$); 5.15, 4.76 (2s, 1.2H, 0.8H, NCH_2CO); 3.67 (s, 3H, OCH_3). *^{13}C NMR (125 MHz, DMSO-d_6, ppm):* δ 167.6, 163.0, 162.7, 162.5, 160.1, 158.5, 152.7, 152.4, 148.7, 145.9, 142.7, 129.7, 129.0, 128.1, 122.7, 122.6, 121.9, 113.5, 107.0, 101.6, 101.4, 55.8, 55.7, 48.2, 47.8. HR-MS (ESI) *m/z* 396.0916 $[M-H]^-$. Anal. Calcd. For $C_{18}H_{15}N_5O_6$ (397.1022): C, 54.41; H, 3.81; N, 17.63. Found: C, 54.49; H, 3.91; N, 17.55.

2.1.10. (E)-N′-(4-Methoxybenzylidene)-2-(7-methyl-4-oxoquinazolin-3(4H)-yl)acetohydrazide (**6b**)

White solid; Yield: 64%. mp: 172–173 °C. R_f = 0.64 (DCM: MeOH = 14: 1). *IR (KBr, cm^{-1}):* 3175 (OH); 3063 (CH aren); 2982, 2939 (CH, CH_2); 1670 (C═O); 1670 (C═N); 1601, 1516 (C═C). *^{1}H NMR (500 MHz, DMSO-d_6, ppm)*: δ 11.73, 11.67 (2s, 0.25H, 0.75H, CONH); 8.33 (2s, 1H, H_2); 8.18, 8.01 (2s, 0.25H, 0.75H, N = CH); 8.05 (dd, *J* = 8.0; *J′* = 3.5 Hz, 1H, H_6); 7.65–7.70 (m, 2H, $H_{2'}$, $H_{6'}$); 7.53 (s, 1H, H_8); 7.40 (d, *J* = 8.0 Hz, H_5); 7.01–7.04 (m, 2H, $H_{3'}$, $H_{5'}$); 3.82 (s, 3H, OCH_3); 5.19, 4.75 (2s, 1.5H, 0.5H, NCH_2CO); 2.49 (s, 1H, CH_3). *^{13}C NMR (125 MHz, DMSO-d_6, ppm):* δ 168.5, 163.7, 161.4, 161.3, 160.6, 149.2, 149.1, 148.7, 147.6, 145.6, 145.5, 144.6, 129.2 129.0, 127.3, 127.1, 127.0, 126.4, 126.3, 119.6, 119.5, 114.8, 55.8, 47.9, 47.3. HR-MS (ESI) *m/z* 349.1272 $[M-H]^-$. Anal. Calcd. For $C_{19}H_{18}N_4O_3$ (350.1379): C, 65.13; H, 5.18; N, 15.99. Found: C, 65.25; H, 5.11; N, 16.10.

2.1.11. (E)-2-(6,7-Dimethoxy-4-oxoquinazolin-3(4H)-yl)-N′-(4-methoxybenzylidene)acetohydrazide (**6d**)

White solid; Yield: 62%. mp: 187–188 °C. R_f = 0.65 (DCM: MeOH = 14: 1). *IR (KBr, cm^{-1}):* 3179 (OH); 3082 (CH aren); 3007, 2943, 2833 (CH, CH_2); 1678 (C═O); 1661 (C═N); 1504 (C═C). *^{1}H NMR (500 MHz, DMSO-d_6, ppm)*: δ 11.71, 11.65 (2s, 0.3H, 0.7H,

CONH); 8.26 (s, 1H, H_2); 8.18, 8.01 (2s, 1.4H, 0.6H, N = CH); 7.70–7.66 (m, 2H, $H_{2'}$, $H_{6'}$); 7.47 (s, 1H, H_8); 7.07–7.02 (m, 2H, $H_{3'}$, $H_{5'}$); 5.19, 4.75 (2s, 1.4H, 0.6H, NCH_2CO); 3.94–3.81 (m, 9H, OCH_3). *^{13}C NMR (125 MHz, DMSO-d_6, ppm):* δ 168.6 162.2 161.3, 160.1, 155.0, 149.3, 147.7, 144.8, 129.2, 129.0, 127.0, 114.9 108.5, 105.6, 56.5, 56.2, 55.8, 47.3. HR-MS (ESI) *m/z* 395.1345 $[M-H]^-$. Anal. Calcd. For $C_{20}H_{20}N_4O_5$ (396.1434): C, 60.60; H, 5.09; N, 14.13. Found: C, 60.71; H, 5.18; N, 14.21.

*2.1.12. (E)-2-(7-Fluoro-4-oxoquinazolin-3(4H)-yl)-N′-(4-methoxybenzylidene)acetohydrazide (**6e**)*

White solid; Yield: 67%. mp: 180–181 °C. R_f = 0.66 (DCM: MeOH = 14: 1). *IR (KBr, cm^{-1}):* 3179 (OH); 3065 (CH aren); 2967, 2907, 2841 (CH, CH_2); 1674 (C═O); 1603 (C═N); 1568 (C═C). *^{1}H NMR (500 MHz, DMSO-d_6, ppm)*: δ 11.74, 11.70 (2s, 0.2H, 0.8H, CONH); 8.43 (2s, 1H, H_2); 8.25–8.18 (m, 1H, H_8); 8.02 (s, 1H, N = CH); 7.70–7.65 (m, 2H, $H_{2'}$, $H_{6'}$); 7.54–7.52 (m, 1H, H_6); 7.47–7.04 (m, 1H, H_5); 7.02, 7.01 (2s, 2H, $H_{3'}$, $H_{5'}$); 5.21, 4.75 (2s, 1.6H, 0.4H, NCH_2CO); 3.82 (s, 3H, OCH_3). *^{13}C NMR (125 MHz, DMSO-d_6, ppm):* δ 168.3, 167.1, 165.1, 163.5, 161.4, 161.3, 160.1, 150.8, 150.7, 150.5, 150.4, 147.7, 144.7, 130.5 129.8, 129.7, 129.2, 129.0, 127.0, 126.9, 119.0, 116.3, 116.1, 114.8, 113.0, 112.8, 55.8, 48.0, 47.5, 47.4. HR-MS (ESI) *m/z* 355.1201 $[M-H]^-$. Anal. Calcd. For $C_{18}H_{15}FN_4O_3$ (354.1128): C, 61.01; H, 4.27; N, 15.81. Found: C, 61.17; H, 4.35; N, 15.75.

*2.1.13. (E)-2-(6-Fluoro-4-oxoquinazolin-3(4H)-yl)-N′-(4-methoxybenzylidene)acetohydrazide (**6f**)*

White solid; Yield: 66%. mp: 181–182 °C. R_f = 0.67 (DCM: MeOH = 14: 1). *IR (KBr, cm^{-1}):* 3283 (NH); 3159 (OH); 3019(CH aren); 2963, 2843 (CH, CH_2); 1676 (C═O); 1653 (C═N); 1603, 1541 (C═C). *^{1}H NMR (500 MHz, DMSO-d_6, ppm)*: δ 11.74, 11.71 (2s, 0.2H, 0.8H, CONH); 8.39 (s, 1H, H_2); 8.19, 8.02 (2s, 0.2H, 0.8H, N = CH); 7.84–7.69 (m, 5H, $H_{2'}$, $H_{6'}$, H_5, H_7, H_8); 7.04, 7.03 (2s, 1.6H, 0.4H, $H_{3'}$, $H_{5'}$); 5.23, 4.79 (2s, 1.6H, 0.4H, NCH_2CO); 3.83 (m, 3H, OCH_3). *^{13}C NMR (125 MHz, DMSO-d_6, ppm):* δ 168.3, 161.3, 160.1, 159.8, 148.6, 145.5, 144.7, 130.6, 130.4, 129.3, 129.0 127.1, 127.0, 123.6, 123.2, 114.8, 111.3, 111.1, 55.8, 47.6. HR-MS (ESI) *m/z* 355.1203 $[M-H]^-$. Anal. Calcd. For $C_{18}H_{15}FN_4O_3$ (354.1128): C, 61.01; H, 4.27; N, 15.81. Found: C, 61.12; H, 4.35; N, 15.73.

*2.1.14. (E)-2-(6-Bromo-4-oxoquinazolin-3(4H)-yl)-N′-(4-methoxybenzylidene)acetohydrazide (**6h**)*

White solid; Yield: 66%. mp: 186–187 °C. R_f = 0.69 (DCM: MeOH = 14: 1). *IR (KBr, cm^{-1}):* 3206 (NH); 3156 (OH); 3064 (CH aren); 2899, 2826 (CH, CH_2); 1705 (C═O); 1663 (C═N); 1605, 1518 (C═C). *^{1}H NMR (500 MHz, DMSO-d_6, ppm)*: δ 11.72 (s, 1H, CONH); 8.43 (s, 1H, H_2); 8.25, 8.15 (2s, 0.6H, 0.4H, N = CH); 8.05–8.00 (m, 2H, H_7, H_5); 7.70–7.60 (m, 3H, $H_{2'}$, $H_{6'}$, H_8); 7.03, 7.02 (2s, 1.2H, 0.8H, $H_{3'}$, $H_{5'}$); 5.22, 4.79 (2s, 1.6H, 0.4H, NCH_2CO); 3.82 (s, 3H, OCH_3). *^{13}C NMR (125 MHz, DMSO-d_6, ppm):* δ 168.2, 163.4, 161.4, 161.3, 159.7, 149.7, 149.6, 147.7, 147.6, 144.7, 137.9, 137.9, 130.2, 129.3, 129.0, 128.6, 128.6, 127.0, 126.9, 123.5, 120.1, 114.8, 55.8, 48.1, 47.6. HR-MS (ESI) *m/z* 415.0399 $[M-H]^-$.

*2.1.15. (E)-N′-(4-(Dimethylamino)benzylidene)-2-(4-oxoquinazolin-3(4H)-yl)acetohydrazide (**7a**)*

White solid; Yield: 63%. mp: 190–191 °C. R_f = 0.62 (DCM: MeOH = 14: 1). *IR (KBr, cm^{-1}):* 3210 (NH); 3069 (CH aren); 2972, 2899, 2816 (CH, CH_2); 1668 (C═N); 1603 (C═N); 1504 (C═C). *^{1}H NMR (500 MHz, DMSO-d_6, ppm)*: δ 11.57, 11.53 (2s, 0.25H, 0.75H, CONH); 8.38, 8.10 (2s, 0.25H, 0.75H, N = CH); 8.18 (d, *J* = 7.0 Hz, 1H, H_5); 7.94 (s, 1H, H_2); 7.87 (t, *J* = 7.0 Hz, 1H, H_6); 7.73 (d, *J* = 8.0 Hz, 2H, $H_{2'}$, $H_{6'}$); 6.76 (d, *J* = 8.0 Hz, 2H, $H_{3'}$, $H_{5'}$); 7.59 (d, *J* = 7.5 Hz, 1H, H_7); 7.55 (d, *J* = 8.5 Hz, 1H, H_8); 5.20, 4.77 (2s, 0.5H, 1.5H, NCH_2CO); 3.35 (s, 3H, CH_3); 2.99 (s, 6H, $N(CH_3)_2$). *^{13}C NMR (125 MHz, DMSO-d_6, ppm):* δ 168.1, 163.2, 160.8, 152.1, 152.0, 149.2, 149.1, 148.6, 145.6, 135.0, 134.9, 129.0, 128.7, 127.7, 127.6, 127.5, 126.5, 122.0, 121.7, 112.3, 48.0, 47.4. HR-MS (ESI) *m/z* 348.1456 $[M-H]^-$. Anal. Calcd. For $C_{19}H_{19}N_5O_2$ (349.1539): C, 65.32; H, 5.48; N, 20.04. Found: C, 65.41; H, 5.37; N, 20.13.

*2.1.16. (E)-N′-(4-(Dimethylamino)benzylidene)-2-(7-methyl-4-oxoquinazolin-3(4H)-yl)acetohydrazide (**7b**)*

White solid; Yield: 63%. mp: 197–198 °C. R_f = 0.63 (DCM: MeOH = 14: 1). *IR (KBr, cm^{-1}):* 3177 (OH); 3063 (CH aren); 2963, 2907 (CH, CH_2); 1668 (C═N); 1603, 1533 (C═C). *^{1}H NMR (500 MHz, DMSO-d_6, ppm)*: δ 11.56, 11.51 (2s, 0.25H, 0.75H, CO-NH); 8.33(s, 1H, H_2); 8.33, 8.09 (2s, 0.25H, 0.75H, N = CH); 8.09–8.03 (m, 1H, H_5); 7.55–7.51 (m, 3H, $H_{2'}$, $H_{6'}$, H_8); 7.40 (d, *J* = 8.0 Hz, 1H, H_6); 6.76–6.74 (m, 2H, $H_{3'}$, $H_{5'}$); 5.17, 4.73 (2s, 1.5H, 0.5H, NCH_2CO), 2.98 (m, 6H, $N(CH_3)_2$); 2.49 (m, 3H, CH_3). *^{13}C NMR (125 MHz, DMSO-d_6, ppm):* δ 168.1, 160.6, 152.0, 149.2, 148.7, 145.5, 145.4, 130.0, 129.0, 128.9, 128.7 127.3, 126.4, 121.7, 119.6, 112.3, 112.2 47.8, 47.3, 21.8. HR-MS (ESI) *m/z* 364.1780 $[M-H]^-$. Anal. Calcd. For $C_{20}H_{21}N_5O_2$ (363.1695): C, 66.10; H, 5.82; N, 19.27. Found: C, 66.17; H, 5.95; N, 19.19.

*2.1.17. (E)-2-(6,7-Dimethoxy-4-oxoquinazolin-3(4H)-yl)-N′-(4-(dimethylamino)benzylidene)acetohydrazide (**7d**)*

White solid; Yield: 57%. mp: 193–194 °C. R_f = 0.65 (DCM: MeOH = 14: 1). *IR (KBr, cm^{-1}):* 3173 (OH); 3082 (CH aren); 2968, 2805 (CH, CH_2); 1670 (C═N); 1605, 1531, 1504 (C═C). *^{1}H NMR (500 MHz, DMSO-d_6, ppm)*: δ 11.55, 11.50 (2s, 0.3H, 0.7H, CONH); 8.33 (s, 1H, H_2); 7.93 (s, 1H, N = CH); 7.55, 7.51 (2s, 1.4H, 0.6H, $H_{2'}$, $H_{6'}$); 7.16 (d, *J* = 8.0 Hz, 2H, H_5, H_8); 6.77, 6.76 (2d, 1.4, 0.6H, $H_{3'}$, $H_{5'}$); 5.11, 4.72 (2s, 0.6H, 1.4H, NCH_2CO); 3.93 (s, 6H, OCH_3); 2.98 (s, 6H, $N(CH_3)_2$).*^{13}C NMR (125 MHz, DMSO-d_6, ppm):* δ 168.2, 164.5, 163.3 160.3 152.1, 152.0, 150.9, 149.8, 149.7, 148.5, 145.5, 128.9, 128.7, 128.2, 121.7, 117.1, 115.4, 112.3, 108.8, 56.3, 47.7, 31.2. HR-MS (ESI) *m/z* 408.1663 $[M-H]^-$. Anal. Calcd. For $C_{21}H_{23}N_5O_4$ (409.1750): C, 61.60; H, 5.66; N, 17.10. Found: C, 61.71; H, 5.55; N, 17.23.

*2.1.18. (E)-N′-(4-(Dimethylamino)benzylidene)-2-(7-fluoro-4-oxoquinazolin-3(4H)-yl)acetohydrazide (**7e**)*

White solid; Yield: 65%. mp: 190–191 °C. R_f = 0.67 (DCM: MeOH = 14: 1). *IR (KBr, cm^{-1}):* 3123 (OH); 3067 (CH aren); 2968, 2897, 2814 (CH, CH_2); 1668 (C═O); 1605, 1504 (C═C). *^{1}H NMR (500 MHz, DMSO-d_6, ppm)*: δ 11.56, 11.52 (2s, 0.25H, 0.75H, CONH); 8.42 (s, 1H, H_2); 8.25–8.22 (m, 1H, H_8); 8.09, 7.94 (2s, 0.25H, 0.75H, N = CH); 7.56–7.43 (m, 4H, $H_{2'}$, $H_{6'}$, H_5, H_6); 6.77–6.74 (m, 2H, $H_{3'}$, $H_{5'}$); 5.19, 4.75 (2s, 1.5H, 0.5H, NCH_2CO); 2.98 (s, 6H, $N(CH_3)_2$). *^{13}C NMR (125 MHz, DMSO-d_6, ppm):* δ 167.9 167.1, 165.1, 163.1, 160.1, 152.1, 152.0, 150.8, 150.7, 150.6, 150.5, 148.6, 145.6, 129.8, 129.7, 129.0, 128.7, 121.7, 119.0, 116.3, 116.1, 112.9, 112.8, 112.3, 47.9, 47.4. HR-MS (ESI) *m/z* 366.1359 $[M-H]^-$. Anal. Calcd. For $C_{19}H_{18}FN_5O_2$ (367.11445): C, 62.12; H, 4.94; N, 19.06. Found: C, 62.23; H, 5.05; N, 18.96.

*2.1.19. (E)-N′-(4-(Dimethylamino)benzylidene)-2-(6-fluoro-4-oxoquinazolin-3(4H)-yl)acetohydrazide (**7f**)*

White solid; Yield: 63%. mp: 191–192 °C. R_f = 0.66 (DCM: MeOH = 14: 1). *IR (KBr, cm^{-1}):* 3175 (OH); 3067 (CH aren); 2965, 2901 (CH, CH_2); 1667 (C═N); 1535 (C═C). *^{1}H NMR (500 MHz, DMSO-d_6, ppm)*: δ 11.57, 11.54 (2s, 0.2H, 0.8H, CONH); 8.38, 8.37 (2s, 0.2H, 0.8H, H_2); 8.09, 7.93 (s, 0.2H, 0.8H, N = CH); 7.85–7.75 (m, 3H, H_5, H_6, H_8); 7.56, 7.51 (2s, 0.4H, 1.6H, $H_{2'}$, $H_{6'}$); 6.77, 6.74 (2s, 0.4H, 1.6H, $H_{3'}$, $H_{5'}$); 5.20, 4.76 (2s, 1.6H, 0.4H, NCH_2CO); 2.98 (s, 6H, $N(CH_3)_2$). *^{13}C NMR (125 MHz, DMSO-d_6, ppm):* δ 167.9, 163.0, 161.7, 160.1, 159.7, 152.1, 152.0, 148.6, 148.6, 145.6, 145.5, 130.7, 130.6, 129.0, 128.7, 123.5, 123.3, 123.2, 123.1, 121.7, 112.3, 112.2, 111.3, 111.1, 48.0, 47.5. HR-MS (ESI) *m/z* 368.1520 $[M + H]^+$. Anal. Calcd. For $C_{19}H_{18}FN_5O_2$ (367.11445): C, 62.12; H, 4.94; N, 19.06. Found: C, 62.19; H, 4.83; N, 19.17.

Table 1
Cytotoxicity of the compounds against some human cancer cell lines.

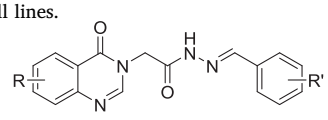

5a-j (R' = 2-OH-4-OCH_3)
6a-h (R' = 4-OCH_3)
7a-h (R' = 4-$N(CH_3)_2$)

Cpd	R	R′	MW	LogP[a]	Cytotoxicity (IC_{50},[b] μM)/Cell lines[c]		
					SW620	PC3	NCI-H23
5a	H	2-OH-4-OCH_3	352.34	1.19	6.10 ± 0.68	8.46 ± 1.28	9.85 ± 1.28
5b	7-CH_3	2-OH-4-OCH_3	366.37	1.74	2.16 ± 0.28	1.48 ± 0.18	1.89 ± 0.13
5c	6-CH_3	2-OH-4-OCH_3	366.37	1.74	2.55 ± 0.21	1.90 ± 0.10	1.74 ± 0.18
5d	6,7-$(OCH_3)_2$	2-OH-4-OCH_3	412.40	0.84	> 10	> 10	> 10
5e	7-F	2-OH-4-OCH_3	370.34	1.40	1.63 ± 0.09	1.31 ± 0.06	1.14 ± 0.03
5f	6-F	2-OH-4-OCH_3	370.34	1.40	1.54 ± 0.29	1.51 ± 0.12	1.35 ± 0.03
5g	6-Cl	2-OH-4-OCH_3	386.79	1.84	1.56 ± 0.03	1.25 ± 0.04	1.75 ± 0.08
5h	6-Br	2-OH-4-OCH_3	431.24	2.08	0.98 ± 0.10	1.30 ± 0.01	1.19 ± 0.07
5i	6-NO_2	2-OH-4-OCH_3	397.34	1.01	3.75 ± 0.58	4.18 ± 0.31	3.58 ± 0.24
5j	7-NO_2	2-OH-4-OCH_3	397.34	1.01	> 10	> 10	> 10
6a	H	4-OCH_3	336.35	0.95	> 10	> 10	> 10
6b	7-CH_3	4-OCH_3	350.37	1.50	> 10	> 10	> 10
6c	6-CH_3	4-OCH_3	350.37	1.50	4.99 ± 0.37	4.22 ± 0.63	4.05 ± 0.31
6d	6,7-$(OCH_3)_2$	4-OCH_3	396.40	0.60	> 10	> 10	> 10
6e	7-F	4-OCH_3	354.34	1.16	> 10	> 10	> 10
6f	6-F	4-OCH_3	354.34	1.16	> 10	> 10	> 10
6g	6-Cl	4-OCH_3	370.79	1.60	2.45 ± 0.03	3.10 ± 0.32	3.34 ± 0.32
6h	6-Br	4-OCH_3	415.25	1.84	> 10	> 10	> 10
7a	H	4-$N(CH_3)_2$	349.39	1.05	5.91 ± 1.41	4.73 ± 0.83	3.01 ± 0.11
7b	7-CH_3	4-$N(CH_3)_2$	363.41	1.60	> 10	> 10	> 10
7c	6-CH_3	4-$N(CH_3)_2$	363.41	1.60	4.68 ± 0.30	4.60 ± 0.33	3.58 ± 0.11
7d	6,7-$(OCH_3)_2$	4-$N(CH_3)_2$	409.44	0.70	> 10	> 10	> 10
7e	7-F	4-$N(CH_3)_2$	367.38	1.25	> 10	> 10	> 10
7f	6-F	4-$N(CH_3)_2$	367.38	1.25	> 10	> 10	> 10
7g	6-Cl	4-$N(CH_3)_2$	383.83	1.70	> 10	> 10	> 10
7h	6-Br	4-$N(CH_3)_2$	428.28	1.94	> 10	> 10	> 10
5-FU[e]			130.08	−0.81	8.84 ± 1.92	13.61 ± 0.46	13.45 ± 3.92
PAC-1			392.49	3.43	4.32 ± 0.34	3.98 ± 0.46	4.09 ± 0.10

[d]Not tested.
[a] Calculated by ChemDraw 9.0 software.
[b] The concentration (μM) of compounds that produces a 50% reduction in enzyme activity or cell growth, the numbers represent the averaged results from triplicate experiments with deviation of less than 10%. Data for **5a, 6c**, **6h, 7c** were reported previously [17].
[c] Cell lines: SW620, colon cancer; PC3, prostate cancer; NCI-H23, lung cancer.
[e] 5-FU: 5-Fluorouracil, a positive control.

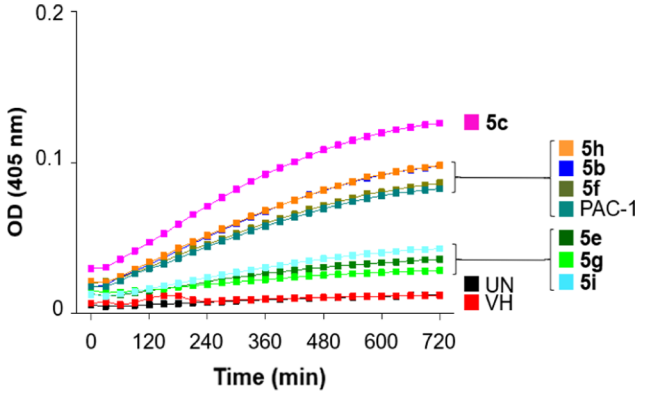

Fig. 3. Caspase-3 activation activity of some representative compounds. U937 human lymphoma cells cells were treated with representative compound (50 μM) for 24 h. Cell lysate was used to detect caspase-3 activation by caspase-3 assay kit. UN: untreated, VH: vehicle (DMSO. 0.05%).

*2.1.20. (E)-2-(6-Chloro-4-oxoquinazolin-3(4H)-yl)-N′-(4-(dimethylamino)benzylidene)acetohydrazide (**7g**)*

White solid; Yield: 68%. mp: 198–199 °C. R_f = 0.65 (DCM: MeOH = 14: 1). *IR (KBr, cm^{-1}):* 3196 (OH); 3125 (CH aren); 2978, 2899, 2818 (CH, CH_2); 1690 (C═O); 166 (C═N); 1533 (C═C). *^{1}H NMR (500 MHz, DMSO-d_6, ppm):* δ 11.55, 11.53 (2s, 0.2H, 0.8H, CONH); 8.42, 8.41 (2s, 0.2H, 0.8H, H_2); 8.11, 8.09 (2s, 0.2H, 0.8H, N = CH); 7.93–7.90 (m, 2H, H_5, H_8); 7.77 (d, *J* = 8.0 Hz, 1H, H_6); 7.56–7.51 (m, 2H, $H_{2'}$, $H_{6'}$); 6.77–6.74 (m, 2H, $H_{3'}$, $H_{5'}$); 5.20, 4.76 (2s, 1.6H, 0.4H, NCH_2CO); 2.99 (s, 6H, $N(CH_3)_2$). *^{13}C NMR (125 MHz, DMSO-d_6, ppm):* δ 167.8, 159.8, 152.0, 149.6, 147.3, 145.7, 135.1, 131.9, 130.1, 129.0, 128.7, 125.5, 123.2, 121.7, 112.3, 47.6. HR-MS (ESI) *m/z* 382.1069 $[M-H]^-$. Anal. Calcd. For $C_{19}H_{18}ClN_5O_2$ (383.1149): C, 59.45; H, 4.73; N, 18.25. Found: C, 59.53; H, 4.88; N, 18.14.

*2.1.21. (E)-2-(6-Bromo-4-oxoquinazolin-3(4H)-yl)-N′-(4-(dimethylamino)benzylidene)acetohydrazide (**7h**)*

White solid; Yield: 66%. mp: 207–208 °C. R_f = 0.63 (DCM: MeOH = 14: 1). *IR (KBr, cm^{-1}):* 3198 (NH); 3121 (OH); 2976, 2899, 2820 (CH, CH_2); 1690 (C═O); 1672 (C═N); 1607, 1535 (C═C). *^{1}H NMR (500 MHz, DMSO-d_6, ppm):* δ 11.56, 11.54 (2s, 0.2H, 0.8H, CONH); 8.43, 8.42 (2s, 0.2H, 0.8H, H_2); 8.25–8.08 (m, 1H, N = CH); 8.08–8.01 (m, 1H, H_5); 7.93 (s, 1H, H_8); 7.69 (d, *J* = 8.5 Hz, 1H, H_6); 7.55–7.51 (m, 2H, $H_{2'}$, $H_{6'}$); 6.77–6.74 (m, 2H, $H_{3'}$, $H_{5'}$); 5.20, 4.76 (2s, 1.6H, 0.4H, NCH_2CO); 2.98 (s, 6H, $N(CH_3)_2$). *^{13}C NMR (125 MHz, DMSO-d_6, ppm):* δ 167.8, 162.9, 159.7, 152.1, 152.0, 149.8, 149.7, 148.6, 147.6, 145.7, 137.8, 130.2, 129.0, 128.7 128.6, 128.5, 123.5,

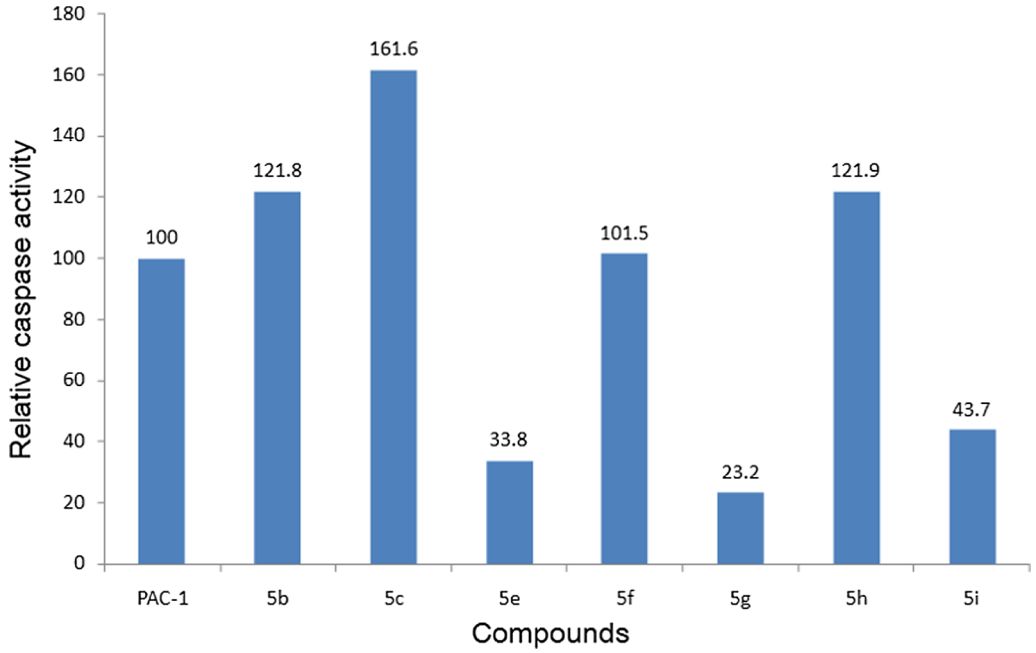

Fig. 4. Relative caspase-3 activation activity of some compounds in comparison to PAC-1. Compounds were tested at 50 μM.

121.6, 120.1, 120.0, 112.3, 48.1, 47.6. MS (ESI) *m/z* 427.9 $[M + H]^+$. Anal. Calcd. For $C_{19}H_{18}BrN_5O_2$ (427.0644): C, 53.28; H, 4.24; N, 16.35. Found: C, 53.37; H, 4.33; N, 16.28.

2.2. Cytotoxicity assay

The cytotoxicity of the synthesized compounds was evaluated against three human cancer cell lines, including SW620 (colon cancer), PC3 (prostate cancer), and NCI-H23 (lung cancer). The cell lines were purchased from a Cancer Cell Bank at the Korea Research Institute of Bioscience and Biotechnology (KRIBB). The media, sera and other reagents that were used for cell culture in this assay were obtained from GIBCO Co. Ltd. (Grand Island, New York, USA). The cells were culture in DMEM (Dulbecco's Modified Eagle Medium) until confluence. The cells were then trypsinized and suspended at 3×10^4 cells/mL of cell culture medium. On day 0, each well of the 96-well plates was seeded with 180 μl of cell suspension. The plates were then incubated in a 5% CO_2 incubator at 37 °C for 24 h. Compounds were initially dissolved in dimethyl sulfoxide (DMSO) and diluted to appropriate concentrations by culture medium. Then 20 μl of each compounds' samples, which were prepared as described above, were added to each well of the 96-well plates, which had been seeded with cell suspension and incubated for 24-h, at various concentrations. The plates were further incubated for 48 h. Cytotoxicity of the compounds was measured by the colorimetric method, as described previously [18] with slight modifications [20–23]. The IC_{50} values were calculated using a Probits method and were averages of three independent determinations (SD ≤ 10%) [24].

2.3. Caspase-3 activation assay

Caspase activity was measured by using caspase 3 assay kit according to the manufacturer's instructions (abcam, MA, USA). U937 human lymphoma cells (5×10^5/ml per well) were plated in 6-well culture plates and allowed to grow for 24 h. The cells were treated with compounds (50 μM) for 24 h, and then harvested. The harvested cells were washed twice with ice-cold PBS and treated with lysis buffer included in the kit. Cell lysate (100 μg/50 μl) was mixed with 50 μl of 2x reaction buffer and 5 μl of DEVD-*p*-NA substrate as the instruction of caspase-3 assay kit (Abcam, cat. N. ab39401). Fluorescence was measured after one-hour incubation.

2.4. Cell cycle analysis

U937 human lymphoma cells (5×10^5/ml per well) were plated in 6-well culture plates and allowed to grow for 24 h. The cells were treated with compounds (50 μM) for 24 h, and then harvested. The harvested cells were washed twice with ice-cold PBS, fixed in 75% ice-cold ethanol, and stained with propidium iodide (PI) in the presence of RNase at room temperature for 30 min. The stained cells were analyzed for DNA content using a FACScalibur flow cytometer (BD Biosciences, San Jose, CA, USA) and the data were processed using Cell Quest Pro software (BD Biosciences).

2.5. Apoptosis assay

The Annexin V-FITC/PI dual staining assay was used to determine the percentage of apoptotic cells. U937 cells (5×10^5/ml per well) were plated in 6-well culture plates and allowed to grow for 24 h. The cells were treated with compounds (50 μM) for 24 h, and then harvested. The harvested cells were washed twice with ice-cold PBS and incubated in the dark at room temperature in 100 mL of 1 × binding buffer containing 1 μl Annexin V-FITC and 12.5 mL PI. After 15 min incubation, cells were analyzed for percentage undergoing apoptosis using a FACScalibur flow cytometer (BD Biosciences). The data were processed using Cell Quest Pro software (BD Biosciences).

2.6. Docking studies

Molecular Operating Environment version MOE 2009.10 [25] was used to perform the docking studies of synthesized compounds in catalytic domain site of caspase-6 (PDB entry 4FXO) [26]. The docking procedures was similar to those reported recently [22,27], that include removing co-crystal ligand, adding hydrogen atoms, parameter setting, minimizing structure, and fixing charge. The London dG (default) was used as first rescoring function with force field (MMFF94x) refinement, and GBVI/WSA as a second one to estimate the negative binding free energy profile of the complex (kCal/mol) [22]. It is emphasized that for docking caspases, water molecules must be conserved as they are an integral part of allosteric mechanisms [26]. The results of docking experiments could be visualized using Chimera 1.13.1 [27].

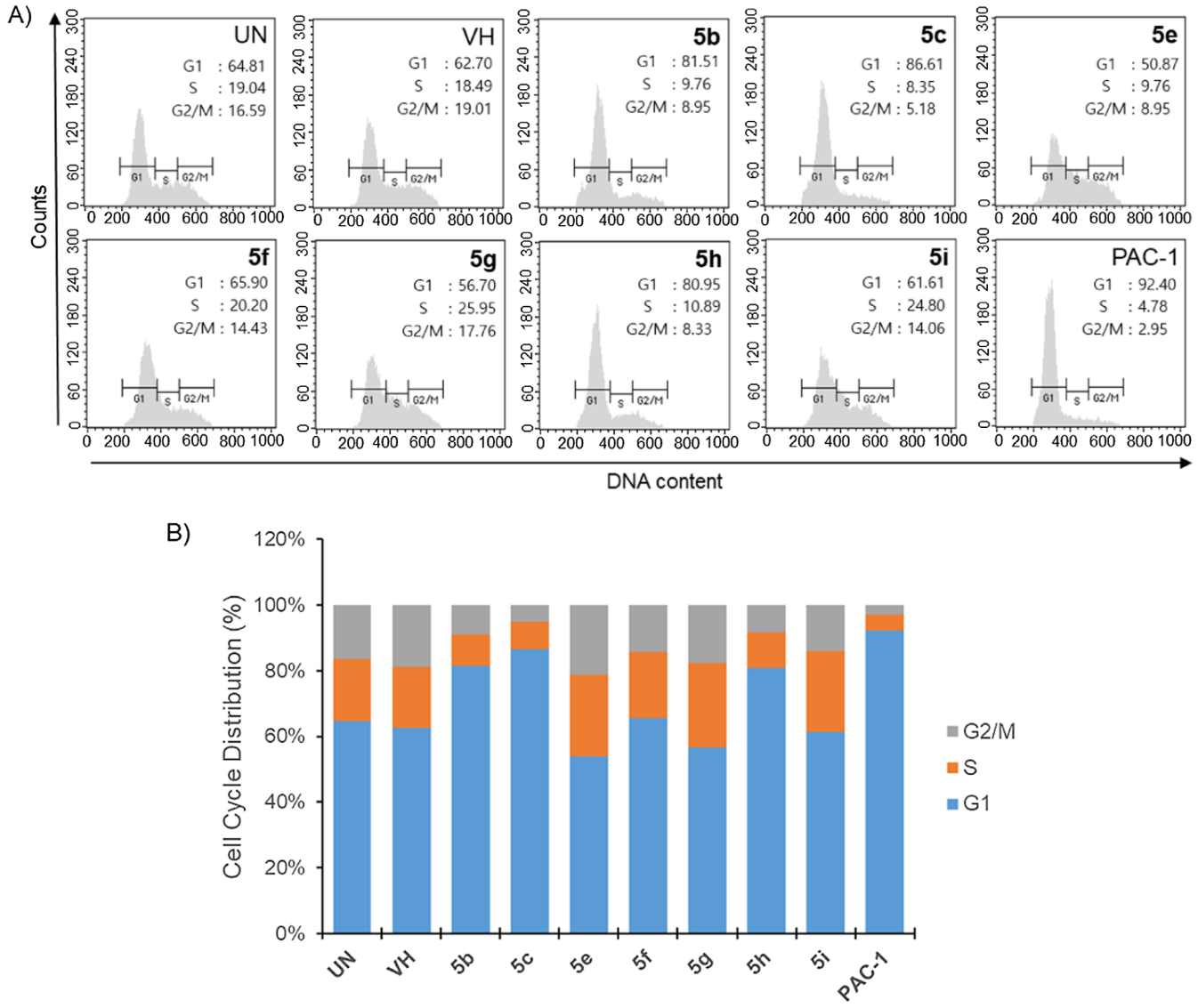

Fig. 5. Cell cycle analysis of some compounds. U937 human lymphoma cells were treated with compounds (50 μM) for 24 h. The harvested cells were stained with propidium iodide (PI) in the presence of RNase and then were analyzed for DNA content. UN: untreated, VH: vehicle (DMSO. 0.05%). Data was represented as histograms (A) and bar graphs (B).

3. Results and discussions

3.1. Chemistry

The designed quinazolin-4(3*H*)-one-based acetohydrazides **(5a-j, 6a-g,** and **7a-h)** were obtained via four step synthetic pathway, as depicted in scheme 1. The first step involved a Niementowski condensation of anthranilic acid (**1a**) or its substituted derivatives (**1b-j**) with an excess of formamide at 120 °C to give the quinazoline-4(3*H*)-ones (**2a-j**) in quantitative yield (89–97%). In the next step, the quinazoline-4(3*H*)-ones (**2a-j**) were reacted with ethyl chloroacetate in acetone with a catalytic amount of KI under basic conditions (K_2CO_3) to give the intermediate esters **3a-j**. Further acyl nucleophilic substitution of the esters **3a-j** with hydrazine monohydrate in ethanol under refluxing conditions afforded the hydrazides **4a-j** at the third step. Finally, an Aldol condensation of the hydrazids **4a-j** with (2-hydroxy-4-methoxy) benzaldehyde, 4-methoxybenzaldehyde or 4-dimethylaminobenzaldehyde furnished the desired products **5a-j, 6a-h,** and **7a-h,** respectively. The target compounds **5a-j, 6a-h,** and **7a-h** were generally obtained in good overall yields.

The structures of the synthesized compounds were determined straightforwardly based on analysis of spectroscopic data, including IR, MS, ^{1}H and ^{13}C NMR. Theoretically, due to enamine tautomerization, the quinazoline-4(3H)-ones (**2a-j**) could react with ethyl chloroacetate to give either or both *N*3- and *O*-alkylated products. However, it has been shown previously that when acetone was used as the reaction solvent, the alkylation reaction gave exclusively *N*3-alkylated products (**3a-j**) [17,28]. The formation of *N*3-alkylated products **3a-j** was demonstrated clearly from ^{1}H and ^{13}C NMR spectroscopic data. In the ^{1}H NMR spectra of the final products (**5–7**), the singlet peaks attributable for two methylene protons generally appeared at around 4.80–5.20 ppm, corresponding to the methylene protons of *N*3-alkylated compounds [17,28]. For the *O*-alkylated products, these methylene protons normally appear more downfield (5.6–5.7 ppm). In the ^{13}C NMR spectra, one peak appeared at around 167–168 ppm was attributable for C=O of the CONHN = functionality. Other peak appeared at around 160–163 ppm was attributable for the carbon of the C_4=O functional group. For the *O*-alkylated products, the peak attributed for a carbon of C_4—O moiety normally appear more downfield than 169 ppm [17,28]. Also, in the O-alkylated products, the carbon of the methylene group was often more downfield, at around 73–77 ppm [17,28], while in the present cases, the methylene carbons generally appeared around

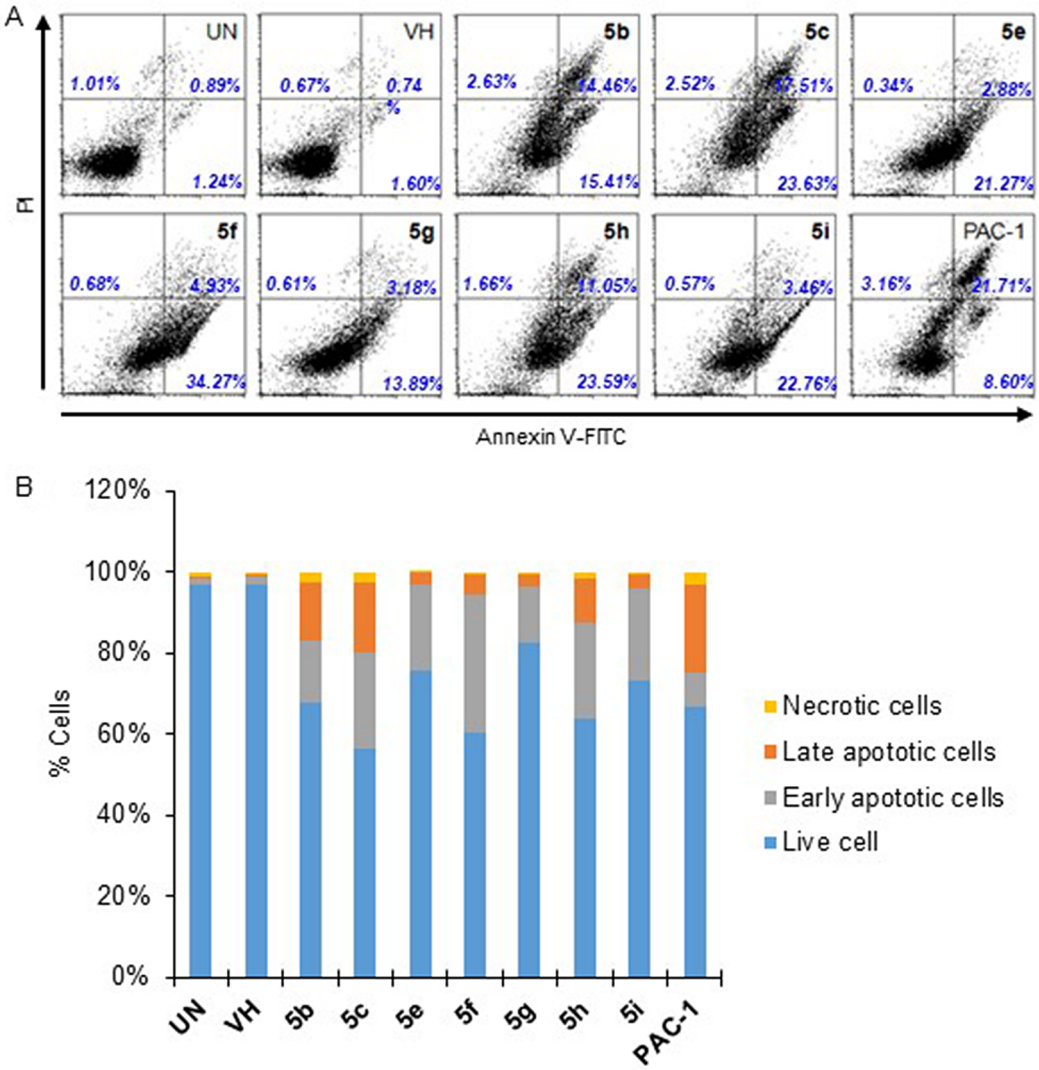

Fig. 6. Apoptosis **(Annexin V/PI)** analysis of some compounds. U937 cells were treated with compounds (50 μM) for 24 h. The harvested cells were incubated with Annexin V-FITC and PI. UN: untreated, VH: vehicle (DMSO. 0.05%). Area 1 = PI positive population, Area 2: Annexin V-postivie population. Data was represented as histograms (A) and bar graphs (B).

46 ppm, which was typical of the methylene carbon attached to N3.

3.2. Bioactivity

Three series of compounds, **5a-j, 6a-h**, and **7a-h**, were firstly evaluated for their cytotoxicity in three human cancer cell lines, including SW620 (human colon cancer); PC3 (human prostate cancer), and NCI-H23 (human lung cancer). 5-Fluorouracil was used as a positive control. PAC-1 was also included in the assay. The results are presented in Table 1.

As can be seen from Table 1, in series **6**, no compound others than compounds **6c** and **6g**, showed significant cytotoxicity in three cancer cell lines tested, up to the concentration of 10 μM. Similarly, in series **7**, only two compounds **7a** and **7c** exhibited moderate cytotoxicity with IC_{50} values in the range between 3.01 and 5.91 μM. Other compounds in the series did not show significant cytotoxicity up to 10 μM against any human cancer cell line assayed. These results indicate that the 4-methoxy and 4-dimethylamino substituents on the phenyl moiety were actually not potential for bioactivity. Only delicate combinations with some appropriate subtituent on the quinazolinone part could afford moderate cytotoxicity, as seen with compounds **6c**, **6g**, **7a** and **7c**.

Interestingly, more potent bioactivity was observed with compounds in series **5a-j**. Although compound **5a**, with no substituent on the quinazolinone part, was found with only moderate cytotoxicity (IC_{50}, 6.10–9.85 μM), most other compounds with 6- or 7-substituted quinazoline rings displayed potent cytotoxicity in all three human cancer cell lines. Both electron releasing groups (such as 6- or 7-methyl substituents) or electron withdrawing groups (e.g. 6- or 7-F, -Cl, -Br) were found to enhance cytotoxicity. In general, electron withdrawing groups seemed to be more favorable for cytoxicity (as seened with IC_{50} values of compounds **5e-h** vs. IC_{50} values of compounds **5b** and **5c**). Regarding the position of the substituents on the quinazoline ring, substitution at position 6 appeared to be more favorable than substitution at position 7, but only in some cases (compound **5i** vs. compound **5j**). The effects of substituent's position was more profoundly noted in series **6** and **7** (compounds **6c** vs. **6b**; compounds **7c** vs. **7b**). A bulky substituent as 6,7-dimethoxy group substantially reduced the compounds's cytotoxicity. Compound **5j** with 7-nitro substituent on the quinazoline moiety was an exception. This compound did not show significant cytotoxicity in all three cancer cell lines up to 10 μM.

In summary, among the three substituents on the phenyl ring of the hydrazone moiety, the 2-OH-4-OCH_3 group was found to be the best substituent for cytotoxicity. This (2-OH-4-OCH_3)-substituted phenyl, in combination with the quinazolinones which were appropriated

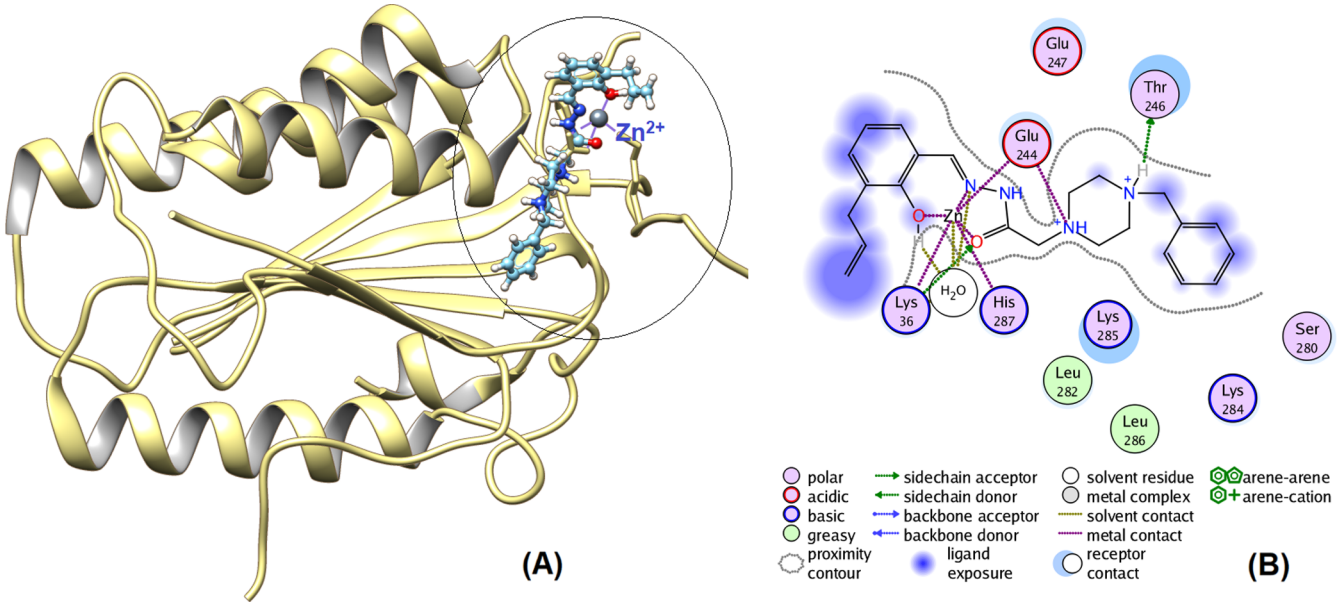

Fig. 7. (A) 3D binding mode of PAC-1 (red molecule) in the allosteric site of caspase-6, and (B) main residues involved in the ligand-protein interactions. Protein is shown as ribbon style, ligand shown as light blue ball and stick style.

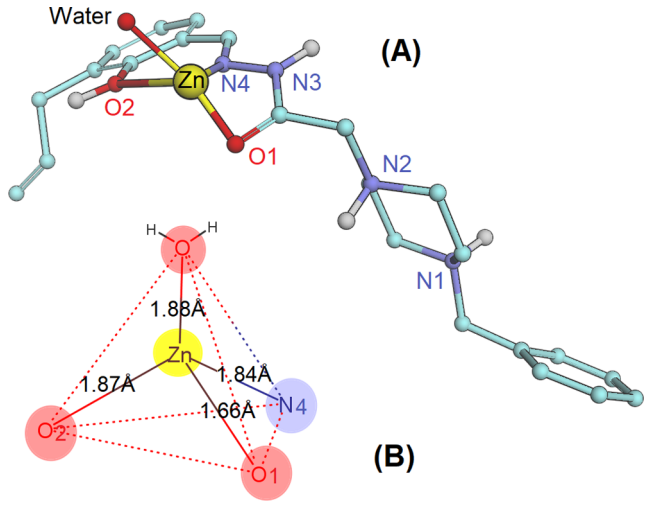

Fig. 8. (A) Molecular structure with atom numberings of docked complex between PAC-1 and Zinc ion (locker of caspase-6). (B) Tetragedral geometry of the corresponding complex.

substituted by small, either electron releasing or electron withdrawing groups at 6- or 7-positions, generally furnished compounds with potent cytotoxicity in three human cancer cell lines (SW-620, PC-3, and NCI-H23). These compounds were almost up to 10-fold more potent than 5-FU and about 2–3 fold more potent than PAC-1. From these results we selected 7 compounds, including **5b. 5c**, and **5e-i** for further evaluation in a caspase-3 activation assay. The results illustrated in Figs. 3 and 4 show that compounds **5h** and **5b** were slightly more potent than PAC-1, meanwhile compound **5f** was equally potent as PAC-1. Three compounds **5e, 5g** and **5i** were less potent than PAC-1 in caspase-3 activation. Very notheworthy, compound **5c** was found to be approximately 1.6-fold more potent than PAC-1 in this assay. This compound was the most potent caspase activator in the series.

SRB assay indicated that series **5**, especially **5b**, **5c**, and **5h**, might induce strong cytotoxicity against cancer cells. We next used flow cytometry to analyze the effects of series **5** on the cell cyles. We treated U937 cancer cells with 50 μM of series **5** for 24 h and then analyzed DNA content and observed that compounds **5b**, **5c**, and **5h** significantly arrested the cell cycle in G1 phase (Fig. 5). We next performed an Annexin V-FITC/propidium iodide (PI) dual staining assay to confirm whether series **5** can induce apoptosis. Phosphatidylserine locates on the cytosolic (inner) side of the cell membrane, and translocates to the extracellular (outer) surface during early apoptosis. Annexin V has a high affinity for PS, and thus when fluorescently labelled with fluorescein isothiocyanate (FITC), can be used to identify early-stage apoptotic cells. Propidium iodide (PI) is a fluorescent intercalating agent that cannot cross the membrane of live cells. The membranes of cells in the latter stages of apoptosis and dead cells are permeable to PI, and their nuclei stain red. We treated U937 cancer cells with compounds at 50 μM for 24 h and stained the cells with Annexin V-FITC and PI. Compounds **5b**, **5c**, and **5h** significantly increased the percentages of Annexin V-PI-double positive cells, namely latter stage of dead cells (Fig. 6). Instead, Compounds **5e**, **5f**, **5g**, and **5i** significantly increased the percentages of Annexin V-single positive cells, namely early stage of dead cells (Fig. 6). These data demonstrate that compounds **5b**, **5c**, and **5h** might be stronger apoptotic cell death inducers than compounds **5e**, **5f**, **5g**, and **5i**.

3.3. Docking studies

As can be identified from the caspase activation assay, three compounds (**5b**, **5c** and **5h**) were more potent than the reference PAC-1. Their cytotoxicity was also impressive, especially **5h** with IC_{50} of 0.98–1.3 μM in three cell lines, showing up to 3–5 times higher than PAC-1. We therefore we decided to continue investigating the caspase activation mechanism of these compound using molecular docking simulation.

It is expected that our synthesized compounds, as derived from PAC-1 structure, would activate procaspase-3 by chelating inhibitory zinc ion through the key *ortho*-hydroxy-*N*-acylhydrazone functionality, thus allowing procaspase-3 to autoactivate itself to caspase-3 [16]. Unfortunately, it is difficult to directly study this mechanism by docking because up to date, there still lacks a zinc-bound crystal structure for procaspase-3. Therefore, we performed the docking simulations with another executioner caspase structurally homologous to caspase-3, that is caspase-6 locked by Zn^{2+} whose crystal structure was reported by Delgado and Hardy [26]. Although the results may not directly reflect the catalytic mechanism of **5b**, **5c** and **5h** in procaspase-3 activation,

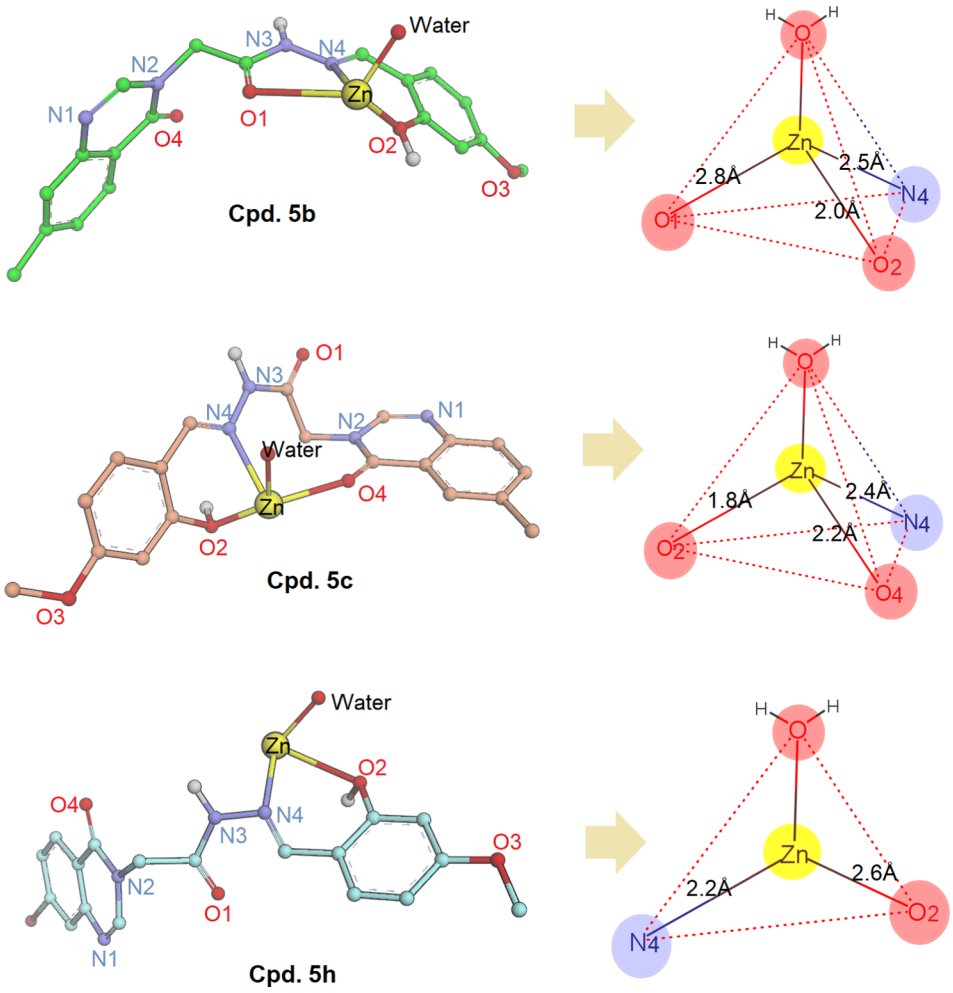

Fig. 9. Metal complex and geometries between **5b**, **5c**, and **5h** with Zinc (extracted from caspase-6 PDB structure ID:4FXO) showing the role of 2-hydroxyl group of the *ortho*-hydroxy *N*-acyl hydrazone moiety in chelating zinc ion.

the docking study could be used, to some extent, to predict the structure-activity relationship related to the zinc binding mode of synthesized compounds which would be useful for rational design and optimization of novel acylhydrazone derivatives in future works.

As for so, all compounds were docked into the allosteric site of caspase-6 for investigating the role of *ortho*-hydroxy *N*-acyl hydrazone motif in chelating zinc ion, and the results were compared with those obtained for PAC-1. As well analyzed, in the central cavity of this enzyme structure, there is a Zn^{2+} ion which exerts its inhibitory role by establishing the tetrahedral geometry with Lys36, Glu244, His287 and water [26,17,18]. The docking results, as shown in Fig. 7, clearly illustrated the chelating mode of PAC-1 to zinc. By penetrate in the allosteric pocket of caspase-6, PAC-1 was able to form a stable complex with zinc ion, with similar coordination geometry as caspase did (Fig. 8). The docking score was determined as −5.03 kCal/mol. It is highlighted the role of *ortho*-hydroxyl group as well as acylhydrazine moiety for forming metal chelation shown in this docking study which is in agreement with those widely reported in literature [29–31].

By applying the same docking procedure for tested compounds, similar results of metal chelation as PAC-1 were observed for **5b**, meanwhile variations were observed for **5c** and **5h** (with a slight variation). All compounds could pertubate the allosteric site in caspase 6 and formed stable tetrahedral coordination with Zn^{2+} and one water molecules. As can be seen in Fig. 9, for compound **5c** the carboxyl group (O4) of 4-oxoquinazoline system played a role in chelating metal; however for **5h** exhibited a bidentate chelation with Zn^{2+} ion *via ortho*-hydroxyl (O2) and amino (N4) groups of acylhydrazine moiety. Among three ligands, the highest possible affinity from a ligand towards the metal, shown by the distance between chelating atoms to the metal and the complexity of the geometry, can be observed in **5c**, suggesting its higher caspase activation ability compared to **5b** and **5h**. This result is correlated with our experimental data given in Fig. 4. Last but not least, in all cases, *ortho*-hydroxyl (O2) group consistently participated in the chelation, reafirming once again the importance of this functionality in sequesting zinc ion as well established in the literature [16,26].

4. Conclusions

In conclusion, we have reported three series of of novel (E)-*N*′-benzylidene-4-oxoquinazolin-3(4*H*)-yl)acetohydrazides (**5a-j, 6a-h,** and **7a-h),** incorporating three different substituents, including 2-OH-4-OCH_3, 4-OCH_3, and 4-$N(CH_3)_2$, respectively, on the phenyl ring of the benzylidene moiety. On the quinazoline part different substituent were introduced at positions 6 and 7. Biological evaluation showed that series (E)-*N*′-(2-hydroxy-4-methoxybenzylidene)-4-oxoquinazolin-3(4*H*)-yl)acetohydrazides (**5a-j**) exhibited the most potent cytotoxicity against three human cancer cell lines (SW620, colon; PC-3, prostate; NCI-H23, lung), while in series **6a-h** and **7a-h** only some compounds were moderately cytotoxic. The cytotoxic potency of compounds 5b, 5c, 5e-i was about 10-fold higher than 5-FU and 2- to 3-fold higher than PAC-1. Small substituents at positions 6 or 7 on the quinazoline moiety, either electron wihthdrawing or releasing, were found to enhance their cytotoxicity. Most of the compounds in this series **5a-j**, especially compounds **5c, 5b** and **5h,** also significantly activated caspase-3

activity. Of these, compound **5c** displayed 1.61-fold more potent than PAC-1 as caspase-3 activator. Cell cycle and apoptotic analyses showed that **5b**, **5c**, and **5h** significantly arrested the cell cycle in G1 phase and these compounds act as as strong apoptotic cell death inducers. The docking simulation studies showed that these compounds could activate procaspase *via* chelating Zn^{2+} ion bound to the allosteric site of the zymogen. From this study we have demonstrated the 2-hydroxy-4-methoxybenzylidene moiety in acetohydrazides appeared to be favorable scaffold for further development of caspase activators and anticancer agents.

Acknowledgements

We acknowledge the principal financial supports from the National Foundation for Science and Technology of Vietnam (NAFOSTED, Grant number 104.01-2018.01). The work was also partly supported by a grant funded by the Korean Government (NRF, Grant number 2017R1A5A2015541).

Declaration of Competing Interest

The authors report no conflict of interest.

References

[1] Y.A. Fouad, C. Aanei, Revisiting the hallmarks of cancer, Am. J. Cancer Res. 7 (5) (2017) 1016–1036.
[2] N.H. Nam, K. Parang, Current targets for anticancer drug discovery, Curr. Drug Targets 4 (2) (2003) 159–179.
[3] S. Storey, Targeting apoptosis: selected anticancer strategies, Nat. Rev. Drug Discov. 7 (2008) 971–972.
[4] S. Lain, J.J. Hollick, J. Campbell, O.D. Staples, M. Higgins, M. Aoubala, A. McCarthy, V. Appleyard, K.E. Murray, L. Baker, A. Thompson, J. Mathers, S.J. Holland, M.J.R. Stark, G. Pass, J. Woods, D.P. Lane, N.J. Westwood, Discovery, in vivo activity, and mechanism of action of a small-molecule p53 activator, Cancer Cell 13 (5) (2008) 454–463.
[5] J.A. Flygare, M. Beresini, N. Budha, H. Chan, I.T. Chan, S. Cheeti, F. Cohen, K. Deshayes, K. Doerner, S.G. Eckhardt, L.O. Elliott, B. Feng, M.C. Franklin, S.F. Reisner, L. Gazzard, J. Halladay, S.G. Hymowitz, H. La, P. LoRusso, B. Maurer, L. Murray, E. Plise, C. Quan, J.-P. Stephan, S.G. Young, J. Tom, V. Tsui, J. Um, E. Varfolomeev, D. Vucic, A.J. Wagner, H.J.A. Wallweber, L. Wang, J. Ware, Z. Wen, H. Wong, J.M. Wong, M. Wong, S. Wong, R. Yu, K. Zobel, W.J. Fairbrother, Discovery of a potent small-molecule antagonist of inhibitor of apoptosis (IAP) proteins and clinical candidate for the treatment of cancer (GDC-0152), J. Med. Chem. 55 (9) (2012) 4101–4113.
[6] A.J. Souers, J.D. Leverson, E.R. Boghaert, S.L. Ackler, N.D. Catron, J. Chen, B.D. Dayton, H. Ding, S.H. Enschede, W.J. Fairbrother, D.C.S. Huang, S.G. Hymowitz, S. Jin, S.L. Khaw, P.J. Kovar, L.T. Lam, J. Lee, H.L. Maecker, K.C. Marsh, K.D. Mason, M.J. Mitten, P.M. Nimmer, A. Oleksijew, C.H. Park, C.-M. Park, D.C. Phillips, A.W. Roberts, D. Sampath, J.F. Seymour, M.L. Smith, G.M. Sullivan, S.K. Tahir, C. Tse, M.D. Wendt, Y. Xiao, J.C. Xue, H. Zhang, R.A. Humerickhouse, S.H. Rosenberg, S.W. Elmore, ABT-199, a potent and selective BCL-2 inhibitor, achieves antitumor activity while sparing platelets, Nat. Med. 19 (2013) 202.
[7] P.M.W. Boudreau, J. Peh, P.J. Hergenrother, Procaspase-3 overexpression in cancer: a paradoxical observation with therapeutic potential, ACS Chem. Biol. (2019), https://doi.org/10.1021/acschembio.9b00338 (in press).
[8] E. Krepela, J. Procházka, X. Liu, P. Fiala, Z. Kinkor, Increased expression of Apaf-1 and procaspase-3 and the functionality of intrinsic apoptosis apparatus in non-small cell lung carcinoma, Biol. Chem. 385 (2) (2004) 153–168.
[9] R. Persad, C. Liu, T.-T. Wu, P.S. Houlihan, S.R. Hamilton, A.M. Diehl, A. Rashid, Overexpression of caspase-3 in hepatocellular carcinomas, Mod. Pathol. 17 (2004) 861–867.
[10] N. O'Donovan, J. Crown, H. Stunell, A.D.K. Hill, E. McDermott, N. O'Higgins, M.J. Duffy, Caspase 3 in Breast Cancer, Clin. Cancer Res. 9 (2) (2003) 738–742.
[11] K.F. Izban, T. Wrone-Smith, E.D. Hsi, B. Schnitzer, M.E. Quevedo, S. Alkan, Characterization of the interleukin-1β-converting enzyme/ced-3-family protease, caspase-3/CPP32, in Hodgkin's disease: lack of caspase-3 expression in nodular lymphocyte predominance Hodgkin's disease, Am. J. Pathol. 154 (5) (1999) 1439–1447.
[12] A. Nakagawara, Y. Nakamura, H. Ikeda, T. Hiwasa, K. Kuida, M.S.S. Su, H. Zhao, A. Cnaan, S. Sakiyama, High levels of expression and nuclear localization of interleukin-1 β converting enzyme (ICE) and CPP32 in favorable human neuroblastomas, Cancer Res. 57 (20) (1997) 4578–4584.
[13] K.S. Putt, G.W. Chen, J.M. Pearson, J.S. Sandhorst, M.S. Hoagland, J.-T. Kwon, S.-K. Hwang, H. Jin, M.I. Churchwell, M.-H. Cho, D.R. Doerge, W.G. Helferich, P.J. Hergenrother, Small-molecule activation of procaspase-3 to caspase-3 as a personalized anticancer strategy, Nat. Chem. Biol. 2 (10) (2006) 543–550.
[14] S.R. Howard, J.H. Paul, Derivatives of procaspase-activating compound 1 (PAC-1) and their anticancer activities, Curr. Med. Chem. 23 (3) (2016) 201–241.
[15] X. Peng, X. Tang, W. Qin, W. Dou, Y. Guo, J. Zheng, W. Liu, D. Wang, Aroylhydrazone derivative as fluorescent sensor for highly selective recognition of Zn2+ ions: syntheses, characterization, crystal structures and spectroscopic properties, Dalton Trans. 40 (19) (2011) 5271–5277.
[16] Q.P. Peterson, D.R. Goode, D.C. West, K.N. Ramsey, J.J.Y. Lee, P.J. Hergenrother, PAC-1 activates procaspase-3 in vitro through relief of zinc-mediated inhibition, J. Mol. Biol. 388 (1) (2009) 144–158.
[17] L.C. Huan, C.V. Phuong, L.C. Truc, V.N. Thanh, H. Pham-The, L.-T.-T. Huong, N.T. Thuan, E.J. Park, A.Y. Ji, J.S. Kang, S.-B. Han, P.-T. Tran, N.-H. Nam, (E)-N'-Arylidene-2-(4-oxoquinazolin-4(3H)-yl) acetohydrazides: synthesis and evaluation of antitumor cytotoxicity and caspase activation activity, J. Enzyme Inhib. Med. Chem. 34 (1) (2019) 465–478.
[18] L.C. Huan, L.C. Truc, C.V. Phuong, P.T. Hai, L.T.T. Huong, N.T.P. Linh, N.T. Thuan, E.J. Park, Y. Choi, J.S. Kang, S.B. Han, N.H. Nam, P.T. Tran, (E)-N'-Arylidene-2-(3-oxo-2,3-dihydro-4H-benzo[b][1,4]oxazin-4-yl)acetohydrazides: synthesis and evaluation of caspase activation activity and cytotoxicity, Chem. Biodivers 15 (10) (2018) e1800322.
[20] Y. Kim, Y.J. You, N.H. Nam, B.Z. Ahn, Prodrugs of 4′-demethyl-4-deoxypodophyllotoxin: synthesis and evaluation of the antitumor activity, Bioorg. Med. Chem. Lett. 12 (2002) 3435–3438.
[21] G. Ye, N.H. Nam, A. Kumar, A. Saleh, D.B. Shenoy, M.M. Amiji, X. Lin, G. Sun, K. Parang, Synthesis and evaluation of tripodal peptide analogues for cellular delivery of phosphopeptides, J. Med. Chem. 50 (2007) 3604–3617.
[22] T.T. Tung, D.T.K. Oanh, P.T.P. Dung, V.T. Hue, S.H. Park, B.W. Han, Y. Kim, J.T. Hong, S.-B. Han, N.H. Nam, New benzothiazole/thiazole-containing hydroxamic acids as potent histone deacetylase inhibitors and antitumor agents, Med. Chem. 9 (2013) 1051–1057.
[23] N.H. Nam, T.L. Huong, D.T.M. Dung, P.T.P. Dung, D.T.K. Oanh, S.H. Park, K. Kim, S.B. Han, Synthesis, bioevaluation and docking study of 5-substitutedphenyl-1,3,4-thiadiazole-based hydroxamic acids as histone deactylase inhibitors and antitumor agents, J. Enz. Inhib. Med Chem. 29 (5) (2014) 611–618.
[24] L. Wu, A.M. Smythe, S.F. Stinson, L.A. Mullendore, A. Monks, D.A. Scudiero, K.D. Paull, A.D. Koutsoukos, L.V. Rubinstein, M.R. Boyd, R.H. Shoemaker, Multidrug-resistant phenotype of disease-oriented panels of human tumor cell lines used for anticancer drug screening, Cancer Res. 52 (11) (1992) 3029–3034.
[25] Molecular Operating Environment (MOE), 2009.10; Chemical Computing Group ULC, 1010 Sherbooke St. West, Suite #910, Montreal, QC, Canada, H3A 2R7; 2009.
[26] E.M. Velázquez-Delgado, J.A. Hardy, Zinc-mediated allosteric inhibition of caspase-6, J. Biol. Chem. 287 (43) (2012) 36000–36011.
[27] E.F. Pettersen, T.D. Goddard, C.C. Huang, G.S. Couch, D.M. Greenblatt, E.C. Meng, T.E. Ferrin, UCSF Chimera–a visualization system for exploratory research and analysis, J. Comput. Chem. 25 (13) (2004) 1605–1612.
[28] M. Špulák, Z. Novák, K. Palát, J. Kuneš, J. Pourová, M. Pour, The unambiguous synthesis and NMR assignment of 4-alkoxy and 3-alkylquinazolines, Tetrahedron 69 (6) (2013) 1705–1711.
[29] S.J. Eron, D.J. MacPherson, K.B. Dagbay, J.A. Hardy, Multiple mechanisms of zinc-mediated inhibition for the apoptotic caspases-3, -6, -7, and -8, ACS Chem. Biol. 13 (5) (2018) 1279–1290.
[30] K.B. Dagbay, J.A. Hardy, Multiple proteolytic events in caspase-6 self-activation impact conformations of discrete structural regions, Proc. Natl. Acad. Sci. USA 114 (38) (2017) E7977.
[31] J. Ma, D. Chen, K. Lu, L. Wang, X. Han, Y. Zhao, P. Gong, Design, synthesis, and structure–activity relationships of novel benzothiazole derivatives bearing the ortho-hydroxy N-carbamoylhydrazone moiety as potent antitumor agents, Eur. J. Med. Chem. 86 (2014) 257–269.

Further reading

[19] P. Skehan, R. Storeng, D. Scudiero, A. Monks, J. McMahon, D. Vistica, J.T. Warren, H. Bokesch, S. Kenney, M.R. Boyd, New colorimetric cytotoxicity assay for anticancer-drug screening, J. Natl Cancer Inst. 82 (13) (1990) 1107–1112.